Mashhadi_MSC

by Nooshin Mashhadi

Submission date: 31-May-2021 12:30PM (UTC+0300)
Submission ID: 1597720255
File name: NOOSH_N_thesis_20210530_turnitin2.docx (7.67M)
Word count: 19745
Character count: 114942

ISTANBUL TECHNICAL UNIVERSITY ★ GRADUATE SCHOOL OF SCIENCE ENGINEERING AND TECHNOLOGY

EVALUATING BFAST ALGORITHM IN LANDSAT TIME SERIES ANALYSIS OF MONITORING DEFORESTATION DYNAMICS IN CONIFEROUS AND DECIDUOUS FORESTS: A CASE STUDY ON MARMARA REGION, TURKEY

M.Sc. THESIS

Nooshin Mashhadi

Department of Applied Informatics

Geographical Information Technology Programme

JUNE 2021

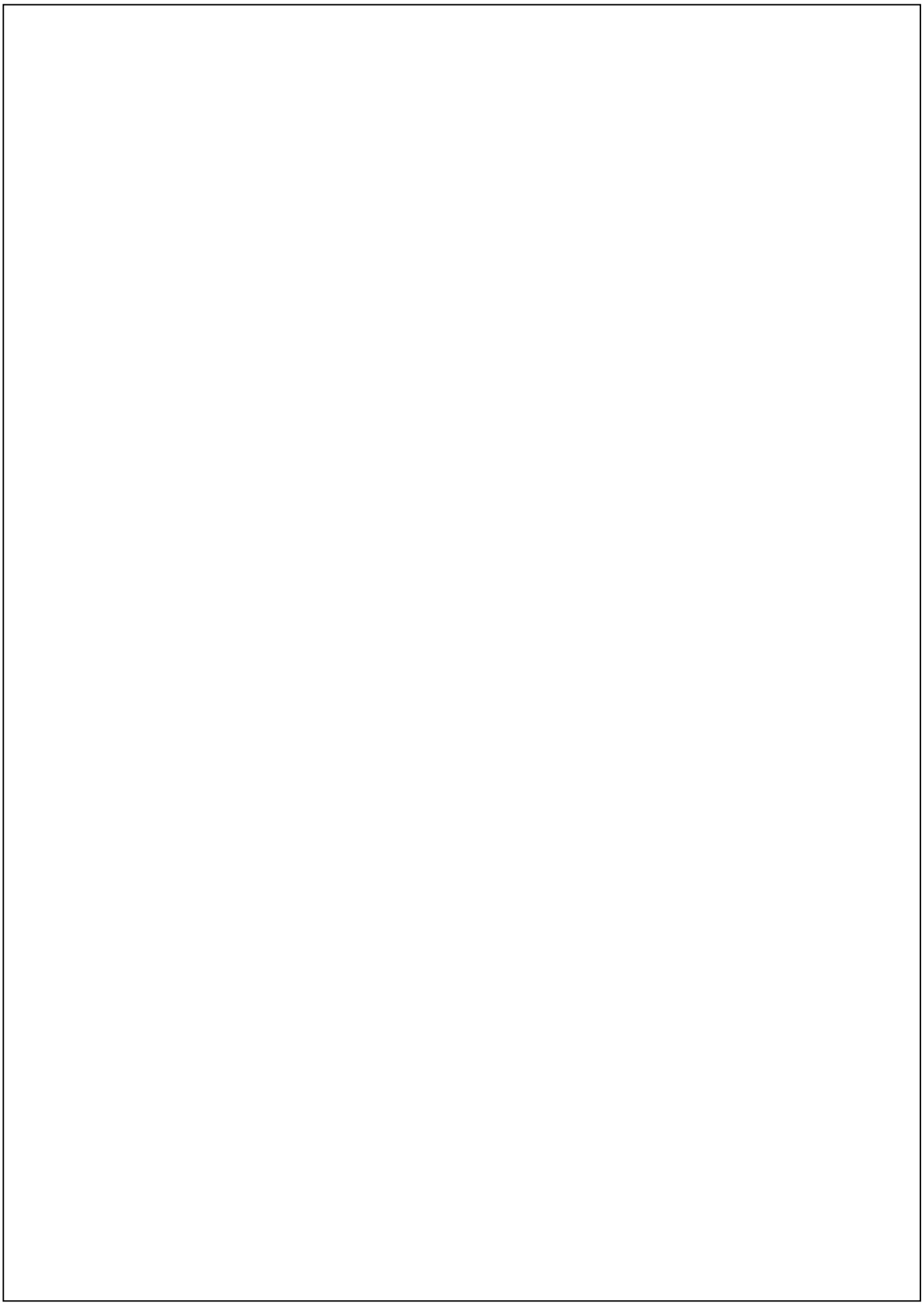

ISTANBUL TECHNICAL UNIVERSITY ★ GRADUATE SCHOOL OF SCIENCE ENGINEERING AND TECHNOLOGY

EVALUATING BFAST ALGORITHM IN LANDSAT TIME SERIES ANALYSIS OF MONITORING DEFORESTATION DYNAMICS IN CONIFEROUS AND DECIDUOUS FORESTS: A CASE STUDY ON MARMARA REGION, TURKEY

M.Sc. THESIS

Nooshin MASHHADI
(706191015)

Department of Applied Informatics

Geographical Information Technology Programme

Thesis Advisor: Assist. Prof. Dr. Uğur ALGANCI
Thesis Co-Advisor: Prof. Dr. Name SURNAME

JUNE 2021

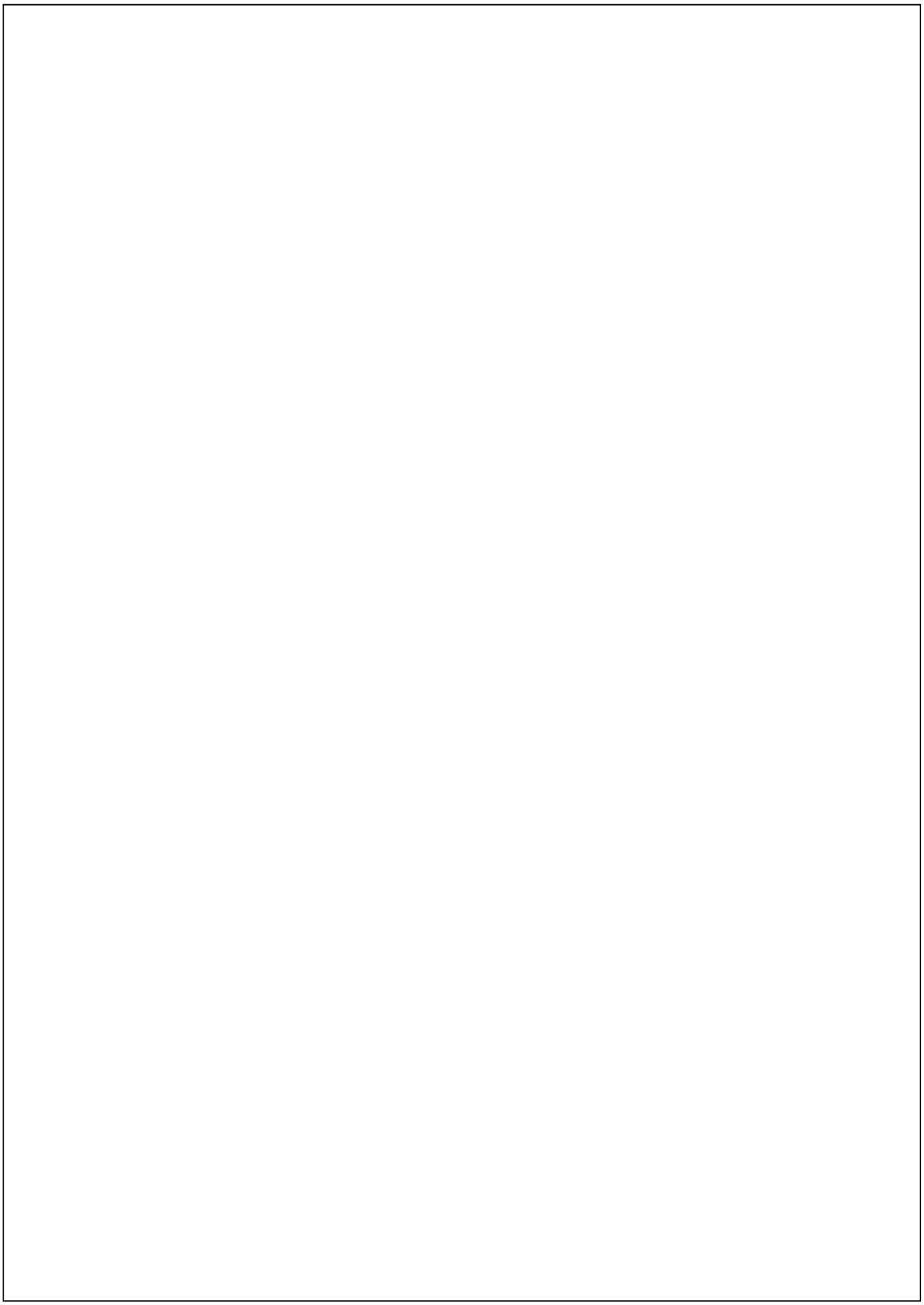

ISTANBUL TEKNİK ÜNİVERSİTESİ ★ LİSANSÜSTÜ EĞİTİM ENSTİTÜSÜ

LANDSAT ZAMAN SERİSİ İLE İĞNE VE GENİŞ YAPRAKLI ORMANLARDA ORMANSIZLAŞMA DİNAMİKLERİNİN İZLENMESİNDE BFAST ALGORİTMASININ DEĞERLENDİRİLMESİ:MARMARA BÖLGESİ; TÜRKİYE ÖRNEĞİ

YÜKSEK LİSANS TEZİ

Nooshin MASHHADI
(706191015)

Bilişim Uygulamaları Anabilim Dalı
Coğrafi Bilgi Teknolojileri Programı

Tez Danışmanı: Doç. Dr. Uğur ALGANCI
(Varsa) Eş Danışman: Doç. Dr. Ad SOYAD

2021

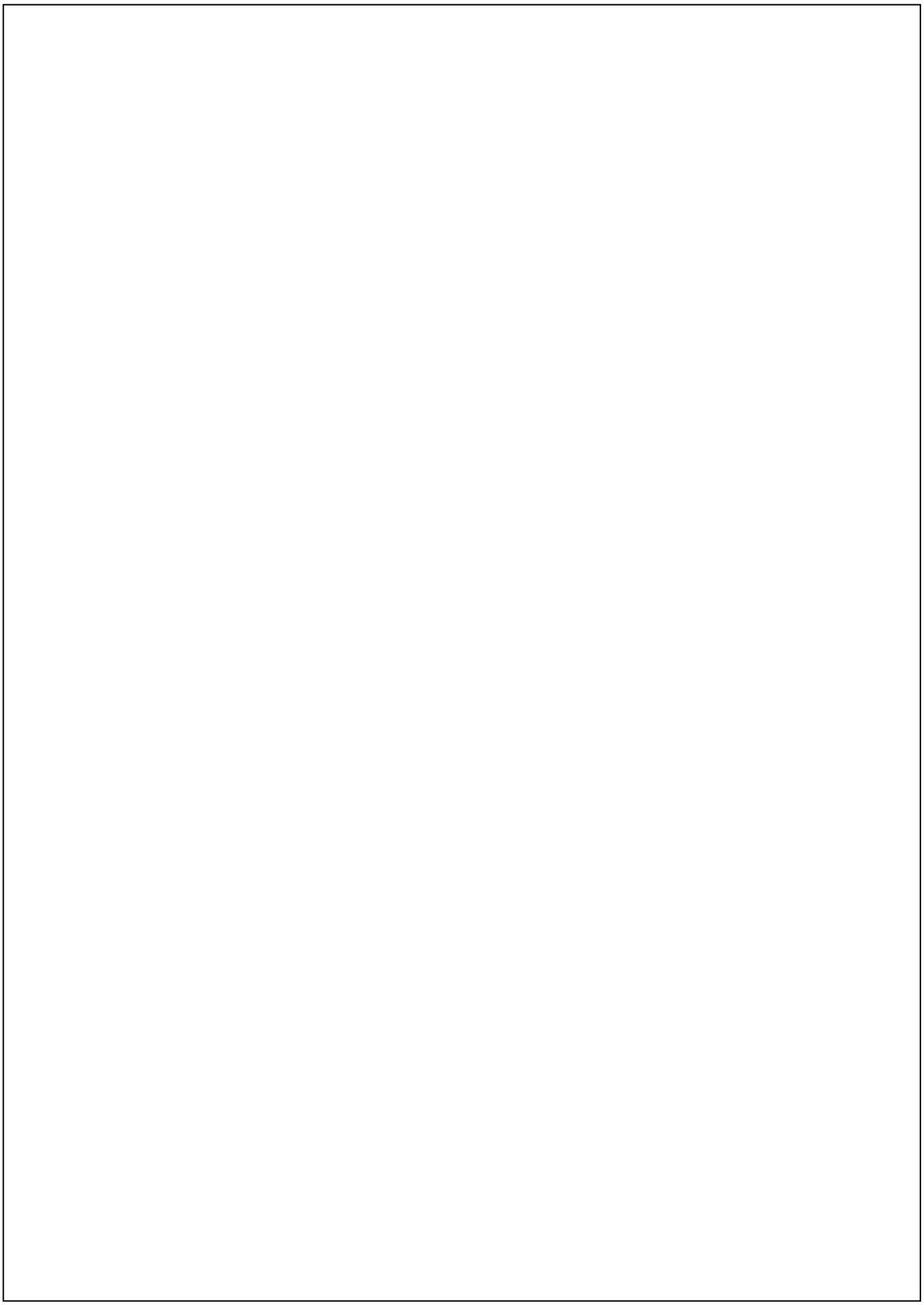

Nooshin Mashhadi, a M.Sc. student of İTU Graduate School of Science Engineering and Technology student ID 706191015, successfully defended the thesis/dissertation entitled "EVALUATING BFAST ALGORITHM IN LANDSAT TIME SERIES ANALYSIS OF MONITORING DEFORESTATION DYNAMICS IN CONIFEROUS AND DECIDUOUS FORESTS: A CASE STUDY ON MARMARA REGION, TURKEY", which she prepared after fulfilling the requirements specified in the associated legislations, before the jury whose signatures are below.

Thesis Advisor :	**Assoc. Prof. Dr. Uğur ALGANCI** İstanbul Technical University	.....
Co-advisor : **(If exists)**	**Prof.Dr. Name SURNAME** ..... University	.....
Jury Members :	**Prof. Dr. Name SURNAME** Istanbul Technical University	.....
	Prof. Dr. Name SURNAME ..... University	.....
	Prof. Dr. Name SURNAME ..... University	.....
(If exists)	**Prof. Dr. Name SURNAME** ..... University	.....
(If exists)	**Prof. Dr. Name SURNAME** ..... University	.....

Date of Submission : 17 December 2014
Date of Defense : 21 January 2015

To me,

FOREWORD

Altering a dream to a real experience is defined by three main steps which are ask, performe, and receive. Passing these three magical steps would definitely create a chance to be triumphed in all level of life. More especifically, being a scientist means always anticipate novel things and never seek to one probable solution, for that reason, having a great and expert mentor in this journey is vitally important. During my M.Sc. study in Istanbul Technical University I had a chance to have Assoc. Prof. Dr. Ugur ALGANCI as my supervisor. He not only guided me through the hard times but also provided me having access to the laboratory of remote sensing of Istanbul Technical University. Assoc. Prof. Dr. Ugur ALGANCI always was available for me both whether having an online meeting or face-to-face meeting, revise my work step by step and inspired me for whole time. I am deeply appreciate my dear supervisor Assoc. Prof. Dr. Ugur ALGANCI for all of these inspirations and encouragements.

I would like to express my sincere thanks to Prof. Dr. Dursun Zafer ŞEKER. I cannot explain in any word how much I am thankful for all of his favors to me as a professor in the class and as the best mentor for accomplishing my goals. Prof. Dr. Dursun Zafer ŞEKER provided me the ambition and the knowledge to keep goinng on my dreams.

Lastly, completing my thesis would not be possible without my friends' helps and encouragements.

June 2021 Nooshin MASHHADI

TABLE OF CONTENT

page

ABBREVIATIONS xiii

LIST OF TABLES xv

LIST OF FIGURES xvii

SUMMARY xix

ÖZET xxii

i

1. INTRODUCTION 1

1.1 Deforestation and Forest Degradation 3
1.2 Deforestation and Biodiversity 3
1.4 Forest Monitoring From Space 4
1.5 Remote Sensing and GIS in Forest Monitoring 4
1.5.1 The efficiency aspects of satellite images in deforestation 5
1.6 Change Monitoring Algorithms 7
1.6.1 Threshold-based change detection 7
1.6.2 Harmonic model 7
1.6.3 BFAST analysis 9

2. LITERATURE REVIEW 11

3. BFAST THEORY IN DETAIL 15

3.1 BFASTMonitor and BFASTspatial 18

4. MATERIALS AND METHODOLOGY 19

4.1 Study Area and Project Context 19
4.1.1 Euxine–Colchic deciduous forests 19
4.1.2 Anatolian conifer and deciduous forests 20
4.2 Data Acquisition and Preprocessing 23
4.2.1 Satellite data 24
4.2.2 Image preprocessing 25
4.3 Vegetation indices 25
4.3.1 Normalized Difference Vegetation Index (NDVI) 28
4.3.2 Enhanced vegetation Index (EVI) 29
4.3.3 Normalized Difference Moisture Index (NDMI) 29
4.3.4. Normalized Burn Ratio (NBR) 30
4.4 Analysis Environment 30
4.5 Analysis Framework 31

4.6 Reference data and Accuracy Assessment 35

5. RESULT AND DISCUSSION 37

5.1 Breakpoints and Magnitude 37
5.2 Accuracy Assessment 41
5.3 The Source of Error in Implementation of BFAST 44
5.4 Discussion 46

6. CONCLUSION 47

REFERENCES 49

APPENDICES 61

CURRICULUM VITAE 68

ABBREVIATIONS

AOI	: Area Of Interest
BFAST	: Break For Additives Seasonality and Trend
CCDC	: Continuous Change Detection and Classification
CRAN	: Comprehensive R Archive Network
EMS	: Electro-Magnetic Spectrum
ETM	: Enhanced Thematic Mapper
EVI	: Enhanced Vegetation Index
FAO	: Food and Agriculture Organization
GEE	: Goofle Earth Engine
GIS	: Geographical Information System
HLS	: Harmonized Landsat-8 and Sentinel-2
LAI	: Leaf Area Index
LiDAR	: Light Detection And Ranging
LTS	: Landsat Time Series
LULC	: Land Use Land Cover
MODIS	: Moderate Resolution Imaging Spectrometer
MSAVI	: Modified Soil-Adjusted Vegetation Index
MSI	: Multispectral Instrument
NA	: Not Applicable
NBR	: Normalized Burn Ration
NDMI	: Normalized Difference Moisture Index
NDVI	: Normalize Difference Vegetation Index
NIR	: Near Infra-Red
OA	: Overall Accuracy
OLI	: Operational Land Imager
PA	: Producer's Accuracy
QA	: Quality Assessment
RADAR	: Radio Detection and Ranging
SAVI	: Soil-Adjusted Vegetation Index
SLC	: Scan Line Corrector
SWIR	: Short Wave Infra-Red

TIR : Thermal Infra-Red

TIRS : Thermal Infra-Red Sensor

TLS : Terrestrial Lasr Scanning

UA : User's Accuracy

USGS : United State Geological Survey

VCF : Vegetation Continuous Field

VCT : Vegetation Change Tracker

VHR : Very High Resolution

VI : Vegetation Index

VNIR : Visible Near Infra-Red

LIST OF TABLES

Page

Table 4. 1: Bands information of Landsat 8 OLI. ..... Error! Bookmark not defined.
Table 5. 1: Pixel percentages of VIs for the study area A.....**38**
Table 5. 2: Pixel percentages of VIs for the study area B.....**39**
Table 5. 3: The accuracy assessment of NDVI for site A.....**42**
Table 5. 4: The accuracy assessment of NDMI for site A. **42**
Table 5. 5: The accuracy assessment of NBR for site A.....**42**
Table 5. 6: The accuracy assessment of EVI for site A. **42**
Table 5. 7: The accuracy assessment of NDVI for site B. **42**
Table 5. 8: The accuracy assessment of NDMI for site B.....**43**
Table 5. 9: The accuracy assessment of NBR for site B.....**43**
Table 5.10: The accuracy assessment of EVI for site B.....**43**

LIST OF FIGURES

Page

Figure 1.1: Comparison between spectral bands among Landsat 8 OLI, Landsat 7 ETM+, and Sentinel 2 (https://landsat.gsfc.nasa.gov/wp-content/uploads/2015/06/Landsat.v.Sentinel-2.png).....**6**

First ordered harmonic model fitted to the Landsat pixels observations by DeVries (2015), indicating seasonal monitoring approach for detecting break (Red line).....**16**

Error! Reference source not found......**17**

Figure 4. 1: Euxine–Colchic deciduous forests (Istanbul natural park).....**20**

Figure 4. 2: Anatolian conifer and deciduous forests (View of Uludağ from Sarıalan). ..... Error! Bookmark not defined.

Figure 4. 3: Location of two study areas. A) Euxine–Colchic deciduous forests over Isanbul B) Anatolian conifer and deciduous forests over Çanakkale province. ..... Error! Bookmark not defined.

Figure 4. 4: Example of EM spectral signiture of healthy vegetation with absorption and reflectance. ..... Error! Bookmark not defined.

Figure 4. 5: Indication of forest canopy reflectance received by passive optical sensors. (A) complete forest, (B)degraded forest with canopy gap, (C) cleared forest, (D) regrowing forest. The bottom thematic of pixels illustrates the impact of different land surface and profile reflectance on a hypothetical vegetation index over 30-meter Landsat data pixels (B DeVries, 2015).....**28**

Figure 4. 6: Folder architecture that needs to be created outside of R environment on the computer. **31**

Figure 4. 7: Methodology diagram, applied to detect breakpoints in time series of landsat vegetation indices from 2015-2020 monitoring period. BFASTSpatial generates a map with the location of breakpoints labeled by date; a map of breakpoints per year labeled by a map of breakpoints per year labeled by month and a map of breakpoints labeled by change magnitude.....**34**

Magnitude values for all detected breakpoints in study area A.....**38**

Error! Reference source not found......**39**

Error! Reference source not found......**40**

Error! Reference source not found......**41**

Error! Reference source not found......**45**

Error! Reference source not found......**45**

EVALUATING BFAST ALGORITHM IN LANDSAT TIME SERIES ANALYSIS OF MONITORING DEFORESTATION DYNAMICS IN CONIFEROUS AND DECIDUOUS FORESTS: A CASE STUDY ON MARMARA REGION, TURKEY

SUMMARY

Forest resources for most of the individual countries have been known as significant resources to provide food, water, wood products, minerals, medicines, etc., to support not only the fundamental facilities for human survival but also economic survival. More specifically, it is proved that in recent years the rate of forest loss due to human-induced or natural disasters has been increased globally. In this regard, having a practical and precise method to prohibit or control deforestation would be necessary.

Countries such as Turkey, hosts different type of forest ecologies, various kind of animal and plant species due to their favorable climate conditions. Protection of forest ecosystems in these countries should be considered as a priority. The most significant reasons for deforestation in Turkey include urban expansion, human construction, agriculture, and fire. In this regard, finding the efficient and accurate method or algorithm for predicting the probable deforestation from the historical data and producing the probable map to prevent future loss in forest resources is crucial.

Changes on the Earth's surface are usually detected by assessing the satellite images as time series, for the same place. There are several criteria to define the suitable sensors for the investigation of different target study areas and different problem definitions. These criteria include spatial, temporal, and spectral resolution of satellite and availability of data. Moreover, apart from satellites' characteristics, phenological characteristic of the land should be considered as it plays prominent role to provide an accurate result of land surface change detection.

Time series analysis with combination of remote sensing provides the opportunity to study abrupt changes, due to serious and strict disturbances, such as deforestation, agriculture, fires, and constructions, as well as gradual changes such as climate variability and forest degradation in the ecosystem. The precision of any change

detection analysis is highly dependents upon the ability of separation among actual changes and fluctuation in seasonal scale.

One of the efficient methods in this context is using the Breaks For Additive Seasonal and Trend (BFAST) set of algorithms, which indicated promising results to detect deforestation areas not only on large scale but on small scale. This method invented according to the time series of Moderate Resolution Imaging Spectrometer (MODIS) satellite data and in recent years indicated accurate results by using Landsat time-series data. Landsat data with more than 40 years of archive data and 30 m spatial resolution becomes an efficient image collection for resolving the entire range of forest disturbances. Medium-to-high resolution Landsat satellite series, since 1972 consistently collecting data from the Earth's surface, facilitated investigation natural resources and the environment. Free availability of Landsat data at 8-16 day intervals at 30m resolution and approximately high temporal resolution with aggregation of comparatively high spatial resolution, proved the effectiveness of Landsat for mapping forest cover and relevant changes.

BFAST iteratively decomposes time series into trend, seasonal, and noise or remainder components. It can deal with missing data without any requirement of interpolation techniques. Using BFAST with a variety of spectral vegetation indices can provide an oppurtunity in detecting changes and deforestation monitoring over different vegetated regions.

BFAST provides the major opportunity to investigate studies on patterns and key changes related to land cover and land use over the duration of time. This method is based on regression modeling of historic observations, fitted on preprocessed data and predict according to the stable harmonic model of historical period in which the remainder data would be compared with the harmonic model. Among different approaches for time series analysis, using spectral indices is pervasive as a result, in BFAST algorithm, geophysical variables are spectral indices, which are dimension-less and demonstrate changes on the land surface such as Normalize Difference Vegetation Index (NDVI), Normalized Difference Moisture Index (NDMI), Normalized Burn Ratio (NBR), Soil-Adjusted Vegetation Index (SAVI), Modified Soil-Adjusted Vegetation Index (MSAVI), Enhanced Vegetation Index (EVI). With respect to the statistical characteristics of each of these indices there is the possibility to conduct time series analysis for a long period to evaluate changes in these indices.

In the concept of time series analysis, having access to the time-series satellite image in perfect atmospheric conditions is vitally important. Clouds and cloud shadows are known as significant obstacle of BFAST method, because cloud masking lead to elimination of several pixels in the images which has a direct impact on the accuracy of the result. Another consern in this algorithm is the numbers of accessible images during the period of study which are related to temporal resolution of selected satellite images. Hence, it is one of the important factors to provide a smooth seasonality during historical period and as a result achieve an accurate prediction during monitoring period.

The general objective of this thesis was to evaluate the feasibility and efficiency of automated time series analysis such as BFAST set of algorithms in R statistical analysis programming language for detecting and monitoring deforestation using Landsat time-series satellite data over deciduous and coniferous types of forest in Marmara region of Turkey.

For this purpose, four different vegetation indices (NDVI, EVI, NDMI, and NBR) were selected as inputs of BFAST set of algorithms. Using various available set of tools of BFAST, time-series stack for each vegetation index was provided. In the next step breakpoints and magnitudes of them calculated to indicate the detection of deforested spots over each study area. The accuracy assessment of the results was performed by collecting stratified random points over the brekpoints magnitude maps of staudy areas. The evaluation of the accuracy was achieved according to the well-known accuracy assessment metrics such as overall accuracy, user's accuracy, producer's accuracy, and bias.

The results demonstrated that BFAST time series analysis tools provided promising results in accurate determination of deforestation. According to results vegetation indices that utilize shortwave infrared bands prove to be more sensitive to detect forest disturbance than the other indices, using red and near-infrared bands. It has been found that the vegetation indices related to water absorption portions of the electromagnetic spectrum such as NDMI and NBR are more sensitive to the changes of forest canopy compared to vegetation indices associated with the chlorophyll absorption, which are calculated with the Red and NIR bands such as NDVI and EVI. In addition, moderate to negative magnitude values proved to be determining the area of deforestation with values, widely varied over different study areas.

The method, discussed in this thesis can produce a map to acquire probable deforestation, correlated to the lowest amount of magnitude class to help better understanding of land cover dynamics and protect forest resource and biodiversity around the world.

LANDSAT ZAMAN SERİSİ İLE İĞNE VE GENİŞ YAPRAKLI ORMANLARDA ORMANSIZLAŞMA DİNAMİKLERİNİN İZLENMESİNDE BFAST ALGORİTMASININ DEĞERLENDİRİLMESİ:MARMARA BÖLGESİ; TÜRKİYE ÖRNEĞİ

ÖZET

Çoğu ülkelerde orman kaynakları, yiyecek, su, odun ürünleri, mineraller, ilaçlar vb. sağlamak için önemli kaynaklar olarak bilinmektedir. Bu kaynaklar sadece canlıların yaşamlarını sürdürmesi için değil, aynı zamanda ekonomik anlamda da temel olanakları sağlamaktadır. Son yıllarda insan kaynaklı veya doğal afetler nedeniyle kaybedilen orman oranının arttığı bilinmektedir. Bu kapsamda, ormansızlaşmayı kontrol etmek ve önüne geçmek için kullanışlı ve tutarlı bir yönteme sahip olmak gerekli olacaktır.

Ayrıca Türkiye gibi farklı iklim koşullarına sahip oldukları için farklı tipte orman ekolojileri, çeşitli hayvan ve bitki türleri barındıran ülkeler öncelikli olarak ele alınmalıdır. Türkiye'de ormansızlaşmanın en önemli nedenleri kentsel genişleme, inşaat, tarım ve yangındır. Bu bağlamda, etkili ve tutarlı bir yöntem ve algoritmayı bulmak, tarihsel verilerden olası ormansızlaşmayı tahmin etmek ve orman kaynaklarının gelecekte kaybolmasını önlemek için ormanların durumunu mekansal boyutta incelemek ve haritalandırmak önem taşımaktadır. Bu kapsamda etkili yöntemlerden biri, BFAST (Breaks For Additive Seasonal and Trend) algoritma setini kullanmaktır. Bu yöntem yalnızca ormansızlaşan alanları sadece büyük ölçekte değil aynı zamanda küçük ölçekte tespit etmekte de umut verici sonuçlar ortaya koymuştur.

Dünya yüzeyindeki değişiklikler genellikle aynı coğrafi alanı kapsayan uydu görüntülerinin zaman serileri olarak değerlendirilmesiyle tespit edilir. Farklı hedef çalışma alanlarının ve farklı problem tanımlarının incelenmesi için uygun sensörleri tanımlamakta kullanılan birkaç kriter vardır. Bu kriterler, uydunun mekansal, zamansal ve spektral çözünürlüğünü ve verilerin kullanılabilirliğini ifade etmektedir. Uyduların özelliklerinden bağımsız olarak, arazi yüzeyinde meydana gelen değişimlerin doğru bir şekilde belirlenmesinde önemli bir rol oynadığı için arazinin zamansal değişim karakteristikleri de dikkate alınabilmektedir.

Zaman serisi analizinin uzaktan algılama ile birlikte kullanılması, ormansızlaşma, tarım, yangın, yapılaşma ve ayrıca ekosistemde dereceli olarak değişen iklim değişkenliği gibi ciddi ve mutlak karışıklıkların çalışılabilmesine olanak sağlamaktadır. Her değişim tespiti analizinin hassasiyeti gerçek değişimin mevsimsel ölçekteki dalgalanmadan ayrıştırılabilmesine yüksek derecede bağlıdır.

BFAST yöntemi MODIS uydu verilerinin zaman serilerine göre geliştirilmiş olup son yıllarda Landsat zaman serisi verileri üzerinde de kullanılarak tutarlı sonuçlar ortaya koymuştur. 40 yıldan fazla arşiv verileri ve 30 m uzamsal çözünürlüğe sahip Landsat verileri, ormanalara ilişkin olguların analizi için verimli bir görüntü arşivi haline gelmektedir. Orta-yüksek çözünürlüklü Landsat uydu serisi, 1972'den beri sürekli

olarak Dünya yüzeyinden veri toplayarak, doğal kaynakların ve çevrenin araştırılmasını kolaylaştırmıştır. Landsat verilerinin 8-16 günlük zamansal aralıklarla 30m uzamsal çözünürlükle ücretsiz kullanılabilirliği ve nispeten yüksek mekansal ve yüksek zamansal çözünürlüğünün bir araya getirilmesiyle, Landsat'ın orman örtüsünün ve ilgili değişikliklerinin haritalanması için potansiyelnin yüksek olduğu birçok çalışmada ortaya konmuştur.

BFAST, arazi örtüsü ve arazi kullanımı ile ilgili temel değişiklikleri ve değişim modellerini araştırmak için büyük bir imkan sağlamaktadır. Aslında, bu yöntem zaman serilerini yinelemeli olarak trend, mevsimsel ve gürültü veya kalan bileşenlerine ayırır. BFAST, herhangi bir enterpolasyon tekniği gerekmeksizin eksik verilerle başa çıkabilir. BFAST'ın çeşitli spektral bitki örtüsü indeksleri ile kullanılması, farklı bitki örtülü bölgelerde değişikliklerin tespit edilmesi ve ormansızlaşmanın izlenmesinde bir fırsat sağlayabilir.

BFAST, tarihsel gözlemlerin regresyon modellemesine dayanarak, ön işlenmiş verilere uygulanarak ve kalan verilerin harmonik modeli ile karşılaştırılacak şekilde dönemin kararlı harmonik modeline göre tahminler üretebilmektedir. Farklı zaman serisi analizlerinde spektral indisleri kullanmak yaygın bir yöntemdir. BFAST algoritmasında by je fiziksel değişkenler boyutsuz olan ve yer yüzeyindeki değişiklikleri gösteren Normalized Difference Vegetation Index (NDVI), Normalized Difference Moisture Index (NDMI), Normalized Burn Ration (NBR), Soil Adjusted Vegetation Index (SAVI), Modified Soil Adjusted Vegetation Index (MSAVI), Enhanced Vegetation Index (EVI) gibi farklı bitki örtüsü indekslerinin zaman serileri olabilmektedir. Her indisin istatiksel karakteristikleri kullanılarak, uzun periyotlu zaman serisi analizi gerçekleştirilmesi ve bu indisler ile değişikliklerin değerlendirilmesi mümkündür.

Bu bakımdan, uygun atmosferik koşullarda zaman serisi uydu görüntüsüne erişebilmek bu yöntemde önemli bir koşuldur. Bulutlar ve bulut gölgeleri, BFAST yönteminin önemli engeli olarak bilinir, çünkü bulut maskeleme, görüntülerdeki belli bir miktar pikselin ortadan kaldırılmasına yol açarak sonucun doğruluğunu doğrudan etkilemektedir. Bu algoritmadaki diğer bir husus, seçilen uydu görüntülerinin zamansal çözünürlüğü ile analiz periyodu boyunca erişilebilen görüntülerin sayısıdır. Dolayısıyla, tarihsel dönemde sorunsuz bir mevsimsellik sağlamak ve sonuç olarak izleme döneminde doğru bir tahminde bulunmak önemli faktörlerden biridir.

Bu çalışmanın amacı, Maramara bölgesinde bulunan yaprak döken ve kozalaklı türünde ormanlar üzerinde, Landsat zaman serisi uydu verilerini kullanarak ormansızlaşmayı tespit etmek ve izlemek için R istatistiksel analiz programlama dilinde yazılmış BFAST algoritma seti ile otomatik zaman serisi analizinin fizibilitesini ve verimliliğini değerlendirmektir.

Bu amaçla, BFAST algoritma setinin girdileri için dört farklı bitki örtüsü indeksi (NDVI, EVI, NDMI ve NBR) seçilmiştir. BFAST'ın çeşitli mevcut araçları kullanılarak, her bitki örtüsü indeksi için zaman serisi yığını sağlanmıştır. Bir sonraki adımda, her çalışma alanı üzerindeki orman niteliğini kaybetmiş konumların tespiti için belirli referans konumlarda kırılma noktaları ve büyüklükleri hesaplanmıştır. Sonuçların doğruluk değerlendirmesi, çalışma alanlarının büyüklük haritaları üzerinden tabakalı rastgele noktalar toplanarak yapılmıştır. Doğruluk değerlendirmesi,

genel doğruluk, kullanıcının doğruluğu, üreticinin doğruluğu ve BIAS gibi iyi bilinen doğruluk değerlendirme ölçütlerine göre gerçekleştirilmiştir.

Sonuçlara göre BFAST zaman serisi analiz araçlarının ormansızlaşmanın belirlenmesinde umut verici çıktılar ortaya koyduğu belirlenmiştir. Kısa dalga kızılötesi bantları kullanan bitki örtüsü endeksleri, kırmızı ve yakın kızılötesi bantları kullanan diğer endekslere göre orman bozulmasını tespit etmekte daha hassas olduklarını kanıtlamıştır. Özetlemek gerekirse, BFAST temelli ormansızlaşma analizinde, EVI ve NDVI'a kıyasla NBR ve NDMI daha tutarlı sonuçlar vermiştir. SWIR ve NIR bantlarından faydalanan bitki indeksleri kanopi nemliliğine çok daha fazla duyarlıdır, dolayısıyla, özellikle ormansızlaşma yamalarında olmak üzere daha tutarlı bir ormansızlaşma tespiti sağlamaktadırlar. Diğer yandan, kırmızı ve NIR bantlarının kullanışması ile hesaplanan VI'lar NDMI ve NBR'ye kıyasla biraz daha düşük performans sergilemiştir. Ancak bu çok büyük olmayan bir performans farkıdır. Sonuçlar ışığıda, NDMI ve NBR gibi elektromanyetik spektrumun su absorbe miktarı ile ilişkili olan bitki indislerinin klorofil absorbesi ile ilişkili olan ve kırmızı ve NIR bantları kullanılarak hesaplanan NDVI ve EVI gibi indislere kıyasla orman kanopi değişimine daha duyarlı olduğu bulunmuştur.

Buna ek olarak, orta ve negatif büyüklük değerlerinin ormansızlaşma alanını belirlediği ve farklı çalışma alanlarına göre büyük ölçüde değişiklik gösterdiği kanıtlanmıştır. Bu tezde benimsenen yöntem, olası ormansızlaşmayı, en düşük büyüklük sınıfıyla ilişkilendirilmiş bir şekilde elde edilmiş bir harita sunma yöntemi sağlamıştır ve bu teknik harita, arazi örtüsü dinamiklerinin daha iyi anlaşılmasına ve dünyadaki orman kaynaklarının ve biyolojik çeşitliliğinin korunmasına yardımcı olabilecektir.

1. INTRODUCTION

Global deforestation and loss in biodiversity, due to the significant development in industry and economy turn to the major concern (McKinney & Lockwood, 1999; Portillo-Quintero et al., 2015). Moreover, land cover changes induced by human and/or natural disaters lead to major costs of extinction of species (Gillespie et al., 2008). Earth's surface change due to human activities is the major concern, led to climate change and biodiversity loss (Klein Goldewijk et al., 2011). In this regard conducting research to ascertain the spatial exten and the dynomics of land transformation is essential to address such issues and expantion of human existance on the Earth (Wulder and Franklin, 2012). Deforestation and forest degredation are the dominant results of climate change due to human activities and urban expansion. As forest biomass encompasses myriad amount of carbon, deforestation and forest degredation contribute as a considerable human-induced carbon emissions (Alley et al., 2007; van der Werf et al., 2009) into the atmosphere, which is the main reason of climate change in this century.

Remote sensing technique has been known as essential alternative to investigate Earth's surface changes due to the accessibility and accumulation of satellite images especially in recent decades (Wu et al., 2020). The initial common methods, to spatiotemporal analysis of land cover changes are image differencing/ ratioing, principal component analysis, tesseled cap transform, post classification comparison, and change vector analysis (Bruzzone et al., 2004; J. Chen et al., 2011; D. Lu et al., 2004). The main concept behind these methods is to define the differences between two images during two time duration, however the limitation of that kind of change detection methods are the requirements for acquisition images of the same sensors with the same temporal, spatial, and spectral resolution. Apart from appropriate satellite image data collections requirements, the precise setting of threshold value is the second considerable challenging issue in change detection analysis with these early common methods (D. Lu et al., 2004). The scarcity of such kind of surface transformation analysis is that they do not have the capacity to define the magnitude

of change and the logical reason behind that change (Jan Verbesselt, Hyndman, Newnham, et al., 2010; Wu et al., 2020).

It is proved that time series analysis in comparison with other initial methods demonstrates considerable accuracy in abrupt changes such as deforestation detection. Some of the time series based upon change trajectories include: vegetation change tracker, Landtrendr (Huang et al., 2010; Kennedy et al., 2010), using for detecting disturbances and regrowth monitoring (Griffiths et al., 2012; Wang et al., 2021), and continuous change detection and classification algorithm (CCDC) (Zhu & Woodcock, 2014). In fact the CCDC uses all available Landsat images during the time analysis and defines the land cover changes and land cover categories after change detection. One of the current time series analysis method is known as Breaks for Additive Seasonal and Trend (BFAST) with high frequency (e.g. monthly) data, which enables demonstrating the changes with detection of the time of changes and more importantly with the magnitude of them. These properties make BFAST an efficient method in determining the abrupt characteristic of the changes such as deforestation and forest degradation (Boriah, 2010). Among all of the time series based change detection methods, the BFAST demonstrated promising results in detecting changes in different type of land covers such as tropical dry forests (Loïc Paul Dutrieux et al., 2015; Smith et al., 2019), wetland (L. Chen et al., 2014), wildlife nature reserve (Platt et al., 2016), city (Tsutsumida et al., 2013), vegetation (Loïc Paul Dutrieux et al., 2015; Jan Verbesselt et al., 2012a), agriculture (Saxena et al., 2018), savanas (Detsch et al., 2016), vegetation fire detection (Hulley et al., 2014), and abandond energy (Waller et al., 2018).

The main challenge through change detection with time series analysis is to detect land cover change from other phenological vegetation changes. At this point, BFAST decomposites changes through trend seasonal and remainder components iteratively and try to separate phenological changes from land cover changes.

The main objective of this thesis is to evaluate the efficiency and accuracy of BFAST analysis in demonstrating the deforestation in two different types of forests (i.e. conifer and deciduous forests) with use of four vegetation indices. The further aim is to determine the magnitude of change and the type of land cover change after deforestation during the period of seven years.

1.1 Deforestation and Forest Degradation

Two main crucial phenomena that threaten the forests are deforestation and forest degradation. In general, forest degradation is known as the forerunner of deforestation (Asner et al., 2005). According to Food and Agricultural Organization (FAO) forests are defined as areas, covered with trees taller than 5 meters in height and with more than 10% canopy cover. Moreover, for the precision of definition this organization has classified forests into four major categories: natural forests (untouched), modified natural forests (native species, some human traces), semi-natural forests (assisted natural regeneration and plantation of indigenous species) and plantation forests (Global Forest *Resources* Assessment 2015 Desk Reference, 2015). Both natural forests and anthropogenic forest plantations are included in this classiffication of forests (Lund, 2013; Matthews, 2014). Deforestation expresses as the elimination of forest cover to less than 10% compared to its original condition. While there is no common definition for forest degradation, generally it is described as a serious reduction in both tree density and the fraction of forest cover, alternatively, it means the transition from closed or dense forest to the open or divided one (DeFries et al., 2007; Key et al., 2004). Ecological repercussions associated with deforestation include changes in soil composition, erosion, changes in microclimates and biodiversity loss. In addition, the ecological balance of the ecosystem is disappeared, and despite of the use of artificial nutrients, eradication of energy stored in human and nutrients is occurred (Elburz et al., 2018).

1.2 Deforestation and Biodiversity

Deforestation is one of the critical environmental issues around the globe, led to extreme contribution in the loss of biodiversity and carbon sequestration (Portillo-Quintero et al., 2015).

The significance of biodiversity is not encapsulated in aesthetics in nature and accessibility of allure natural resources, but in the context of measuring productivity, broadly, there is a positive correlation between productivity of a forest and species richness (Vilà et al., 2007). In this regard, the loss of biodiversity around the globe is a-major concern in term of biological conservation. Taken together near-real-time monitoring and restoring of residual forests in high biodiversity ecoregion are needed to trigger efficient results to prohibit loss of biodiversity. A plethora of studies have

proved that several decades ago, the vast majority of land areas on the Earth were dedicated to forests. Recently FAO announce that globally 129 million hectares of forests were eradicated either because of human-induced or anthropogenic activities between 1990 and 2015.

1.4 Forest Monitoring From Space

Remote sensing change detection is defined as the procedure of identifying differences between images at different times (Singh, 1989). It plays a prominent role in characterizing human and natural disturbances in forest areas to provide information for managing forest areas. Given that, there are some considerations apparent as major noises, such as seasonal differences due to solar angle differences, and vegetation phenological changes and need to be considered at the stage of opting satellite data. Remote sensing instruments are categorized into two different types either active or passive. In active remote sensing sensors (RADAR sensors) generates their own electromagnetic radiation, measured when reflected back from the Earth's surface while Passive sensors (Optical sensors) assess the solar energy reflected or emitted from the Earth's surface at the wavelengths in visible, near Infrared (NIR), Short-Wave Infrared (SWIR), and Thermal Infrared (TIR) (Peng et al., 2016). Moreover, in active sensors radiations can penetrate through clouds and provide information through areas with high cloud cover. However, both of these sensors have advantages in the field of forest and change detection analysis of land cover. In this thesis, optical sensors have been used due to their wide accessibility to the data and associated methods.

1.5 Remote Sensing and GIS in Forest Monitoring

Remote sensing and Geographical Information System (GIS) play a prominent role in the detection of deforestation from past patterns. Furthermore, satellite images have been widely used for monitoring earth surface and change detection across the world. Remote sensing means acquiring information about the physical characteristics of an object at or near the surface of the Earth by measuring the reflected or emitted radiation through the device typically satellites or spacecrafts that are not in contact with the subject under investigation. In this context remote sensing is useful to provide information that is problematic or infeasible to obtain (D. Lu et al., 2004; Purkis & Klemas, 2013).

Satellite images have the abilitiy to provide large data repositories of vegetation cover for a long period. Earth observation satellite images are widely used to monitoring and facilitating area of deforestation (Coppin et al., 2004; Mas, 1999; Singh, 1989).

GIS has been defined as a system to collect, analyze and retrieve information. It has wide range of application in environmental issues, in the context of deforestation mostly used for the preparation of hot and cold spot analysis, effects of anthropogenic and meteorological aspects and role of digital elevation model in deforested areas to help forest managers and stockholders to make a decision and take steps in respect to prohibit loss of forests (de By et al., 2001).

1.5.1 The efficiency aspects of satellite images in deforestation

During the 21st century Moderate Resolution Imaging Spectrometer (MODIS) have played a key role in change detection analysis, however, due to the relatively coarse spatial resolution of this satellite small and subtle changes have been excluded across the Earth's forest. Therefore Landsat data with more than 40 years of archive data and 30 m spatial resolution becomes an efficient image collection for resolving the entire range of forest disturbances (Cohen et al., 2017). Medium-to-high resolution Landsat satellite series, since 1972 consistently collecting data from the Earth's surface, facilitated investigation natural resources and the environment. Free availability of Landsat data at 8-16 day intervals at 30m resolution and approximately high temporal resolution with aggregation of comparatively high spatial resolution. The Multi-spectral Scanner (MSS) sensors have spectral range from 0.5 to 1.1 μm, indicated visible and Near Infrared (NIR) wavelengths. Thematic Mapper (TM) and Enhanced Thematic Mapper Plus (ETM+) sensors on board Landsat 4, Landsat 5, and Landsat 7 respectively have the wider range of Electromagnetic Spectrum (ELS). It is worth mentioning that the Scan Line Corrector (SLC) on board Landsat 7 failed in 2003 as a result,, after this year all the scenes have lost approximately 22% of data (B DeVries, 2015; Maxwell et al., 2007).

In 2013, US Geological Survey (USGS) launched Landsat 8 with Operational land imager (OLI) sensor, with an expanded spectrum of wavelengths and extra bands in comparison with TM and ETM+ sensors. These features enhanced the ability of OLI in atmospheric correction and cloud masking (Irons et al., 2012; Langner, 2009).

Recently Landsat 9 was introduced and would be launched in September 2021. Landsat 9 will have the broadest spectrum coverage with collecting data in three

Shortwave Infrared (SWIR) bands and two Thermal Infrared (TIR) bands, in addition to visible- Near Infrared (VNIR).

Landsat collections have promoted land-monitoring algorithms whether in seasonal or long-term trends (Brooks et al., 2014; Kennedy et al., 2010; Jan Verbesselt, Hyndman, Newnham, et al., 2010; Zhu & Woodcock, 2014). Moreover, alongside the increasing proportion of Landsat time series (LTS) (Broich et al., 2011; Grecchi et al., 2017; Huang et al., 2010; Kennedy et al., 2010; Zhu & Woodcock, 2012), myriad numbers of studies have proved the effectiveness of Landsat for mapping forest cover and relevant changes (Hansen & Loveland, 2012; Loveland & Dwyer, 2012; Pflugmacher et al., 2014; Roy et al., 2014; Wulder et al., 2012).

Applying high-resolution satellite images, such as those derived from Sentinel-2, have been demonstrated prominent result in change detection analysis. However, converse to the Landsat satellites series Sentinel-2 does not cover images from vast range of time duration as it has launched in 2015. Recently NASA has provided the continuous surface reflectance products of Earth's surface, Harmonized Landsat-8 and Sentinel-2 data (HLS), stemmed from images of Multispectral Instrument (MSI) and Operational Land Observation (OLI) onboard sensors of Sentinel-2 and Landsat-8 satellites respectively (Pastick et al., 2018).

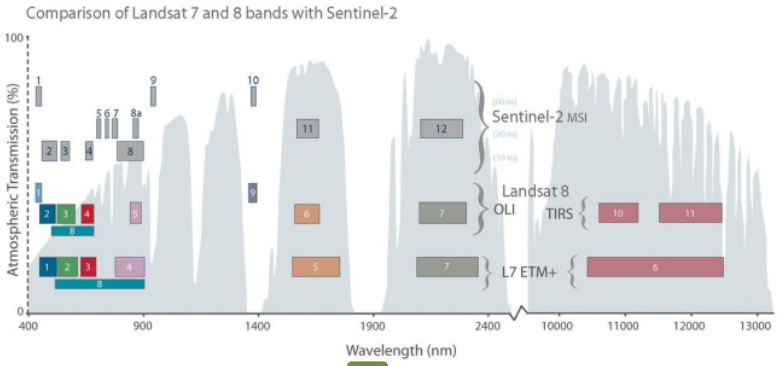

Figure 1.1: Comparison between spectral bands among Landsat 8 OLI, Landsat 7 ETM+, and Sentinel 2 (https://landsat.gsfc.nasa.gov/wp-content/uploads/2015/06/Landsat.v.Sentinel-2.png).

1.6 Change Monitoring Algorithms

Changes on the Earth's surface are usually detected by assessing the satellite images as time series, for the same place. There are several criteria to define the suitable sensors for the investigation of different target study areas and different problem definitions. These criteria include spatial, temporal, and spectral resolution of satellite and availability of data. Moreover, apart from satellites' characteristics, phenological characteristic of the land should be considered as it plays prominent role to provide an accurate result of land surface change detection.

This approach is implemented by supervised or unsupervised classification algorithms to detect every changes pixel basis for the entire scene. The problem with such kind of Land Use Land Cover (LULC) change detection is the misclassification error that reduce the accuracy of algorithm (Mardian, 2020). As a matter of the fact, more direct algorithms have been developed based on the radiometric characteristics of the images.

1.6.1 Threshold-based change detection

Image differencing is one of the ubiquitous change detection techniques due to its simplicity. This method works only by calculating differences between two pixels. There are some concerns related to this method that makes disability to demonstrate all changes on the land surface, contribute to the issue of having not any control on some prominent factors such as solar illumination, sensor calibration and atmospheric conditions (Mardian, 2020).

Equivalently, image ratioing, instead of subtracting two images, aims to detect the changes by using ratios of images. The prosperity of image differencing to image ratioing is the ability to remove noise from the slope, aspect, sollar illumination, and seasonal changes (Berberoğlu et al., 2016; Mardian, 2020). It is important to mention that the barrier of this method is that the source of change cannot be defined as only the magnitude of change is obtained as a result. This method has been widely used for variety of applications such as for grassland monitoring, as it is capable of identifying both abrupt changes and gradual changes.

1.6.2 Harmonic model

The usage of the harmonic model is with cyclical data by breaking a time series, in two or more waveform shape data use number of summation between sinusoidal series.

In terms of deforestation several algorithms can be applied, while one of the most frequently used algorithms with Landsat data collections is the Landsat-based detection of Trends in Disturbance and Recovery (Land Trendr) (Kennedy et al., 2010). This algorithm is used for detecting abrupt changes such as deforestation. Normalized Burn Ratio (NBR) is the main change index in this method. Land Trendr works based on the segmentation method, while a slope is fitted to each segment in respect to demonstrating gradual changes (Zhu, 2017). Another model named, the Vegetation Change Tracker (VCT) (Huang et al., 2010), works based on the thresholding method with a contribution of normalization of each images to demonstrate abrupt changes such as deforestation. Earning this approach is upon of converting each image to forest probability index, called integrated forest z-score. Other applications of VCT including detecting abrupt changes in crop and wet-land (Huang et al., 2010; Sexton et al., 2013; Zhu, 2017). Both Land Trendr and VCT are offline and univariate change detection methods and cannot use for real-time monitoring of land surface (Zhu, 2017). The Continuous Change Detection and Classification (Zhu & Woodcock, 2014) and The Breaks for Additive Season and Trend (BFAST) algorithm (Jan Verbesselt, Hyndman, Newnham, et al., 2010) are near real time algorithm to indicate abrupt changes. These algorithms are based on high frequency type of satellite images (Zhu, 2017). BFAST is encompassed of at least three main components, trend, season, and noise, which make the capability of BFAST to detect both abrupt and gradual changes. Initially this algorithm was based upon MODIS composite time series to demonstrate vegetation change in an offline mode (Jan Verbesselt, Hyndman, Newnham, et al., 2010). After that BFASTMonitor, was developed to detect drought in vegetation in real time by utilizing MODIS time series (Jan Verbesselt et al., 2012b). Recently, BFAST showed the promising result in contribution of Landsat time series data to detect forest changes such as deforestation and fires (B DeVries, 2015; Loïc P. Dutrieux et al., 2016; M. Lu et al., 2017). These exclusive techniques in remote sensing context provide an explicit way to detect changes in surface reflectance to assess trend as remarkable changes in pixel values among spate of satellite images, led to modification of changes in land cover or land use.

Among these algorithms, the most pervasive one in the context of near real time (time series analysis) change detection is the Breaks for Additive Season and Trend

(BFAST) algorithm. Briefly, BFAST can evaluate the number of abrupt changes within time series and describes these changes according to their magnitude and directions. BFAST is an appropriate tool for analyzing different types of time series such as Moderate Resolution Imaging Spectrometer (MODIS) and Landsat (Schultz et al., 2013; Jan Verbesselt et al., 2012a; Jan Verbesselt, Hyndman, Zeileis, et al., 2010).

1.6.3 BFAST analysis

Recently BFAST has been widely used in biotic and abiotic environmental disturbances such as droughts, fires and vegetation changes (Jan Verbesselt, Hyndman, Newnham, et al., 2010; Watts & Laffan, 2014), in both agriculture (Atzberger, 2013) and forested landscapes (Lambert et al., 2013, 2015; Schmidt et al., 2015), confirmed as a reliable tool (Chandra, 2011). Considerably time series analysis with the contribution of related statistical techniques such as BFAST provides the major opportunity to investigate studies on patterns and key changes related to land cover and land use over the duration of time, although in most of the algorithms in change detection analysis just a before and after scenario take into the consideration. Detailed information about BFAST algorithm could be found in Chapter 3.

2. LITERATURE REVIEW

Over the decades, remote sensing techniques have rapidly been advanced. In the field of monitoring and mapping earth surface, two sensors played a more prominent role than others, Moderate to High resolution Imaging Spectroradiometer (MODIS), aboard Terra and Aqua NASA satellites by monitoring the Earth since 2000 and Landsat series of satellites, by collecting information since 1970s. Manual digitization of forest cover by using aerial photography and satellite imagery to provide ground truth information of forest cover is known as an initial stage of deforestation mapping. Trejo & Dirzo (2000), demonstrated early potential vegetation maps to make a comparison between plausible and existing vegetation. This concept needs an enormous effort among both digitizers and analysts to investigate any change detection merely in a few duration of time. However, since the 1970's, this constraint has been diminished due to technological improvements in automated mapping tools and satellite imaging technologies. These developments allowed scientists to map forests over any particular area of the world, assessing the temporal trends of deforestation either annually or across decades.

Time series analysis aim to use an input as series of data, which can be both continuous or discrete, and the values demonstrate observations that collected during the time-sequential (Chatfield et al., n.d.). The aim of time series is to define the variation in the subject of interest within these time intervals and execute the effect such as trend, correlation, cycle or changing behavior. With in the aspect of remote sensing of land cover change, time series analysis defined as temporal analysis of land surface dynamics through the continuous observations and assessment of the trajectory of dependent variables such as geophysical indices or thematic variables (Collins et al., 2018; Jamali et al., 2015; Wohlfart et al., 2016)

Time series analysis with combination of remote sensing provides the opportunity to study abrupt changes, due to serious and strict disturbances, such as deforestation, agriculture, fires, and constructions, as well as gradual changes such as climate

variability and forest degradation in the ecosystem. The precision of any change detection analysis is highly dependents upon the ability of separation among actual changes and fluctuation in seasonal scale (Jan Verbesselt, Hyndman, Newnham, et al., 2010). Among different approaches for time series analysis, using spectral indices is pervasive (Hislop et al., 2018). Spectral indices, such as Normalize Vegetation Index (NDVI), Leaf Area Index (LAI), Normalize Burn Ratio (NBR), are dimensionless geophysical variables that demonstrate changes on the land surface. With respect to the statistical characteristics of each of these indices there is the possibility to conduct time series analysis for a long period to evaluate changes in these indices. Thematic variables can be derived from some approaches such as classification and regression analysis of original values, stack them to gather and interpret the changes during the sequential of time (Tran et al., 2018).

Verbesselt et al. (2010) developed BFAST as the statistical package in R programming language, which stands for Breaks for Additive Seasonal Trends. It is based on a harmonic analysis model for detection changes in time series, for each pixel in the Landsat scene, it fits the best seasonal regression model with a trend component. At the initial stage BFAST was used to demonstrate forest change in southern Australia with respect to Normalized Difference Vegetation Index (NDVI) stem from MODIS, the most frequent type of data for other studies in the field of BFAST (Bullock et al., 2020). The main objective of BFAST is to determine the moment and location of changes during the time series. In this regard, BFAST decomposes time series into three main components, harmonic, trend, and remainder or error term. The aggregation of BFAST and MODIS 250m in various dry tropical forest types using the Normalized Difference Moisture Index (NDMI) (Grogan et al., 2016).

NDVI has been used in several investigations in the context of forest change detection, such as deforestation detection in the boreal forest (Hüttich et al., 2014), clear cut mapping in a temperate forest (Lambert et al., 2015), mixed forest change detection in Australia on hyper-temporal data (Schmidt et al., 2015) and deforestation detection. M. Lu et al. (2016) disclosed BFAST as robust change detection algorithm, in confining changes from temporally and spatially autocorrelated Enhanced Vegetation Index 2 (EVI2) time series across the moist tropical forest. Apart from the application of BFAST in forest change detection, Cai et al. (2016) indicated the capability of

BFAST to measure the flooding of e Yangtze river, additionally Che et al. (2017) assessed the fluctuation of lake size in Tibet.

Verbesselt et al. (2012b) revealed the new domain of BFAST, BFASTMonitor. The novel method was more flexible and robust especially when data are irregular and scares (Reiche et al., 2015). BFASTMonitor performs based on the historical data observations in which it defines their model and make prediction into a monitoring period and observation would be compared to this model. Change magnitude values defined when there is an extreme deviation between observed and modeled value during the monitoring period. Moreover, if this deviation is significant at a specific moment in time, this timing is implemented. Verbesselt et al. (2012b) demonstrated that BFAST indicates accurate results in significant changes whether in gradual or abrupt changes over long time period, and has the capability of eradicating noise or false positive breaks. Although in 2016, Schultz et al. indicated the enormous number of errors related to BFAST algorithm, such as topography, atmosphere, edge effects and data availability and variance. These factors would affect commission errors; however, the availability of data during monitoring time is significant because the number of observations has a prominent effect on accuracy and omission errors. Enormously BFAST Monitor was utilized in the field of deforestation and forest degradation, but there are several investigations, applied this method in other applications such as detection of burned area in a savannah landscape Liu et al. (2018), estimation of forest canopy change (Romero-Sanchez & Ponce-Hernandez, 2017). Potter (2019) used MODIS 250 m NDVI time series as an input for BFAST method to evaluate vegetation changes more specifically due to wildfires over Yellowstone National Park (USA). This study concluded that BFAST can indicate burned spots as well as representing regrowing domains over the study area (Potter, 2019). Recently Wu et al. (2020) implemented BFAST and Landsat NDVI time series in the West Dongting Lake region to investigate conversion from forest to other land cover category, from other land cover category to the forest and from forest to forest due to flooding or reforestation. They demonstrated that BFAST is capable to detect multi-type forest changes with low data availability (Wu et al., 2020). Bueno et al. (2020), used BFAST Monitor in seven different vegetation indices (NDVI, EVI, SAVI, MSAVI, NBR, NBR2, and NDMI) and three distinct domains (Atlantic forest, savanna, and semi-arid woodland) in Brazil to compare provided disturbance maps

and analyze if there is any correlation among them. They concluded that variation in input data leads to producing non-spatially correlated disturbance maps and representing site-specific sensitivity. The aggregation of BFASTMonitor and Google Earth Engine was investigated by (Hamunyela et al., 2020). They used time-series Landsat for NDMI to evaluate their GEE BFAST Monitor implementation to detect forest disturbances in three distinct forest areas, including humid tropical forest, dry tropical forest, and miombo woodland and compare the result with the original BFASTMonitor with R programming language. They ascertained the high amounts of spatial and temporal agreements between the results stemmed from both the original BFASTMonitor and their GEE BFASTMonitor implementations for forest disturbance.

3. BFAST THEORY IN DETAIL

Generally, BFAST iteratively decomposes time series into trend, seasonal, and noise or remainder components. It could be whether utilized for variety of satellite image time series or other subjects such as hydrology, climatology, and econometrics. Algorithm can be applied on seasonal or non-seasonal time series. Moreover, BFAST can deal with missing data without any requirement of interpolation techniques (Jan Verbesselt et al., 2015).

Recently, there are several studies indicated the capability of BFAST algorithm and Landsat time series using a variety of spectral vegetation indices in change detection and deforestation monitoring over different vegetated regions. Among all of them, the most pervasive one is the Landsat time series and NDVI to demonstrate the ability of this spectral index in land degradation and deforestation areas (Bueno et al., 2020b).

Apart from NDVI, other vegetation indices such as EVI, NBR, NDMI, NDFI, indicated their suitability in the application of BFAST. In the context of near real-time monitoring of disturbances such as degradation and deforestation by the utility of BFAST, one of the subdivided of this algorithm, has opened up and it is called BFASTMonitor, provided the ability to monitoring changes in near-real-time approch (Verbesselt et al., 2012b; Schultz, 2018).

This method is based on regression modeling of historic observations, fitted on preprocessed data and perform prediction according to the stable harmonic model of historical period, in which the remainder data would be compared with the harmonic model. BFAST Monitor approximately indicated reasonable result, implementing on Landsat or similar data, characterized by 30 m resolution and irregular observation cycle (Reiche et al., 2015). To detect forest disturbances, we applied a pixel-wise time series method based on the BFAST monitoring approach described in (Jan Verbesselt et al., 2012a). In this thesis, three main approaches would be considered to detect changes for the pixels included in the benchmark forest mask: (1) For the first step a harmonic model according to the observations in the historic period is defined. (2) Testing approach would be performed according to the break from fitting harmonic

model; and (3) Calculating the median of the residuals for all estimated and real observations within the monitoring period. These steps are described in more detail below.

1) Fitting a harmonic model: this model assumes each new pixel in a time series as a historical period and a monitoring period which is defined by $t_i \epsilon [t_1 \; t_N]$; The monitoring period start time at t_n the history period would be defined as $t_1 < t_i < t_n$ and monitoring period as the remainder of the time which is $t_n < t_i < t_N$ (Figure 3.1 by DeVries (2015) shows the demonstration of these variables).

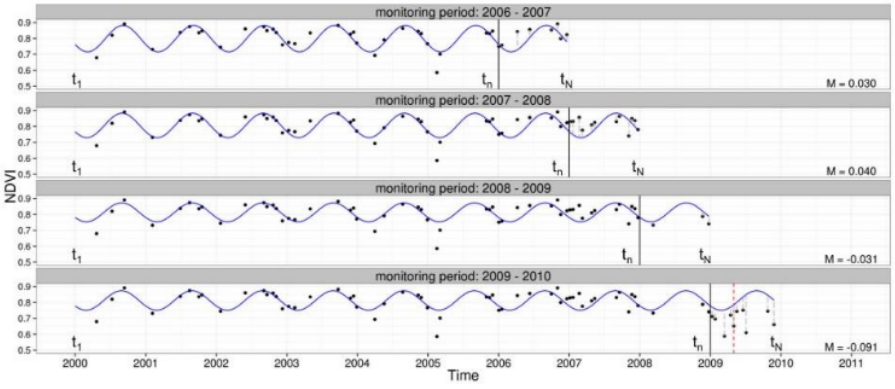

Figure 3.1 : First ordered harmonic model fitted to the Landsat pixels observations by DeVries (2015), indicating seasonal monitoring approach for detecting break (Red line).

It is persumed that the stable forested pixels refer to the begining of the monitoring period (t_n). So according to the Verbesselt et al. (2012b) the first order harmonic model defied, fitting to all observations during history period showed in equation 3.1.

$$y_t = \alpha + \gamma sin\left(\frac{2\pi t}{f} + \delta\right) + \varepsilon_t \qquad (3.1)$$

Where:

y_t is dependent variable

t is independent variable

f is temporal frequency

α is intercept

γ and δ are amplitude and phase of the components respectively

ε_t is the noise components (residual).

2) Detecting change (break points): For detecting significant deviation among pixels during monitoring period from the historical period we used Ordinary Least Square (OLS) moving sum of residuals (MOSUM) using fraction of observation, defined by lag value (h) during historical period.

$$\boldsymbol{MO_t = \frac{1}{\hat{\sigma}\sqrt{n}} \sum_{s=t-h+1}^{t} (y_s - \hat{y}_s)} \quad (3.2)$$

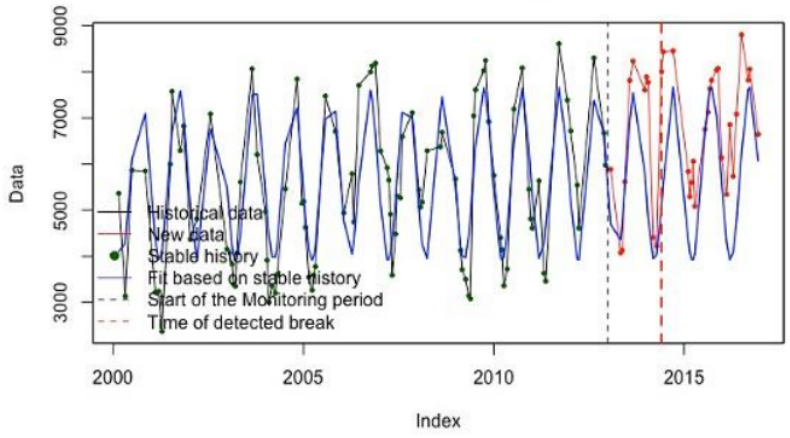

Figure 3.2 : Example of a break point on a single-pixel by BFAST (Break detected at 2014 (149th pixel) (B DeVries, 2015).

Where respectively y and $\hat{y}$ are real and estimated observations, n is the number of sample observations, h is the fraction of number of observation known as the bandwidth of MOSUM during history period (n) Verbesselt et al. (2012b), $\hat{\sigma}$ is the estimator of the variance (B DeVries, 2015; Zeileis et al., 2005). The signal of break point would be defined when deviates from zero to beyond 95% significance boundary (Leische *et al*., 2000). (Figure 3.2)

3) Computing change magnitude: BFAST also provides this opportunity to earn the magnitude of change M during monitoring period $t_n < t_i < t_N$ by calculating the median of residuals Equation 3.3:

$$M = \{\boldsymbol{y_t} - \hat{\boldsymbol{y}}_t\} \quad (3.3)$$

where $\boldsymbol{y_t}$ and $\hat{\boldsymbol{y}}_t$ are real and estimated observations, respectively (B DeVries, 2015).

The vitally important parameters that can be modified by BFAST are listed below. Although; there are other parameters, these are the most significant ones:

- formula – regression model formula (harmonic and/or trend component)
- order – order of the harmonic term
- start – starting date of the monitoring period
- history – specification of the stable history period
- h – Bandwidth relative to the sample size in the MOSUM monitoring process, the numeric between 0-1.

3.1 BFASTMonitor and BFASTspatial

In the context of near real-time monitoring of disturbances such as degradation and deforestation by the utility of BFAST, one of the subdivision of this algorithm, BFAST Monitor has opened up. However, it should be noted that, since BFASTMonitor time-series input is univariate, it cannot be used with raster data input. In this regard, the optimized version "bfmspatial" can accept a raster brick as an input and run "bfastmonitor" for each pixel of an image. Raster brick is an object class in R, encompassed multiple layers, in this case, satellite image layers. The output of "bfmspatial" is a raster brick with layers of break point, magnitude, and error, also there would be supplementary layers such as r.squared, adj.r.squared, and coefficients, but there are not in the scope of this research (Schultz, Verbesselt, et al., 2016; Jan Verbesselt et al., 2012b).

Some studies shown promising results by utilizing the BFAST family algorithm to detect abrupt and gradual phenological changes (Schultz, Clevers, et al., 2016; Jan Verbesselt, Hyndman, Newnham, et al., 2010). In their research conduct, several errors related to BFAST such as topography, atmosphere, edge effects, data availability, and variance were not discussed. In the context of data availability, the density of the data plays an important role on deriving the more accurate result from time series. Recently, due to the wide range of temporal resolution of satelite images and specially the existance of optical satellite missions such as Sentinel-2A & 2B it is feasible to fill the gap during monitoring period of the time series investigations (Schultz, Verbesselt, et al., 2016).

4. MATERIALS AND METHODOLOGY

4.1 Study Area and Project Context

Turkey hosts a significant variety of forest types in its different regions. In this thesis, two different regions of Turkey with different forest types were selected as study regions to evaluate the accuracy of BFASTspatial in detecting deforestation. The detailed information about dominant forest types in these regions are as follow:

4.1.1 Euxine–Colchic deciduous forests

These forests are categorized as temperate broadleaf and mixed forests ecoregion (Figure 4.1). Vegetation ranges from temperate rainforest to coastal bottomland forests, peatlands and coastal sand dunes. This ecoregion is located in southern of Black Sea, extended from the short region in the southeastern of Bulgaria to the northern parts of Turkey to the east of Georgia. The Colchian forests have various kind of tree species, which include, deciduous black alder (Alnus glutinosa), hornbeam (Carpinus betulus and C. orientalis), Oriental beech (Fagus orientalis), and sweet chestnut (Castanea sativa), with combination of evergreen Nordmann fir (Abies nordmanniana, the tallest tree in Europe at 78m), Caucasian spruce (Picea orientalis) and Scots pine (Pinus sylvestris) (Çolak et al., 2011).

Figure 4.1 : Euxine–Colchic deciduous forests (Istanbul natural park).

4.1.2 Anatolian conifer and deciduous forests

These forests are located in the southern part of Marmara Sea region and the western parts of Turkey. The main plant communities of this realm are pure pine forests, mixed pine, oak woodlands, and shrublands. This type includes the oaks Quercus cerris, Q. ithaburensis ssp. macrolepis, and Q. Cocifera (Çolak et al., 2011).

Figure 4.2 : Anatolian conifer and deciduous forests (View of Uludağ from Sarıalan).

Below the location of these two forest areas is demonstrated over the Marmara region of Turkey. The first one is in the northern part of Marmara, indicated Istanbul forest areas and second the western part of Marmara, Canakkale province Figure 4.3.

For the sake of interpreting deforestation two sub-division of these areas were selected to be investigated through BFAST analysis, with more amount of forest land cover changes during the period of study, 2013-2020. In Istanbul the main reason fordeforestation was construction of a new airport (Alganci, 2019), while in Canakkale deforestation was due to the mining activities (Çolak et al., 2011).

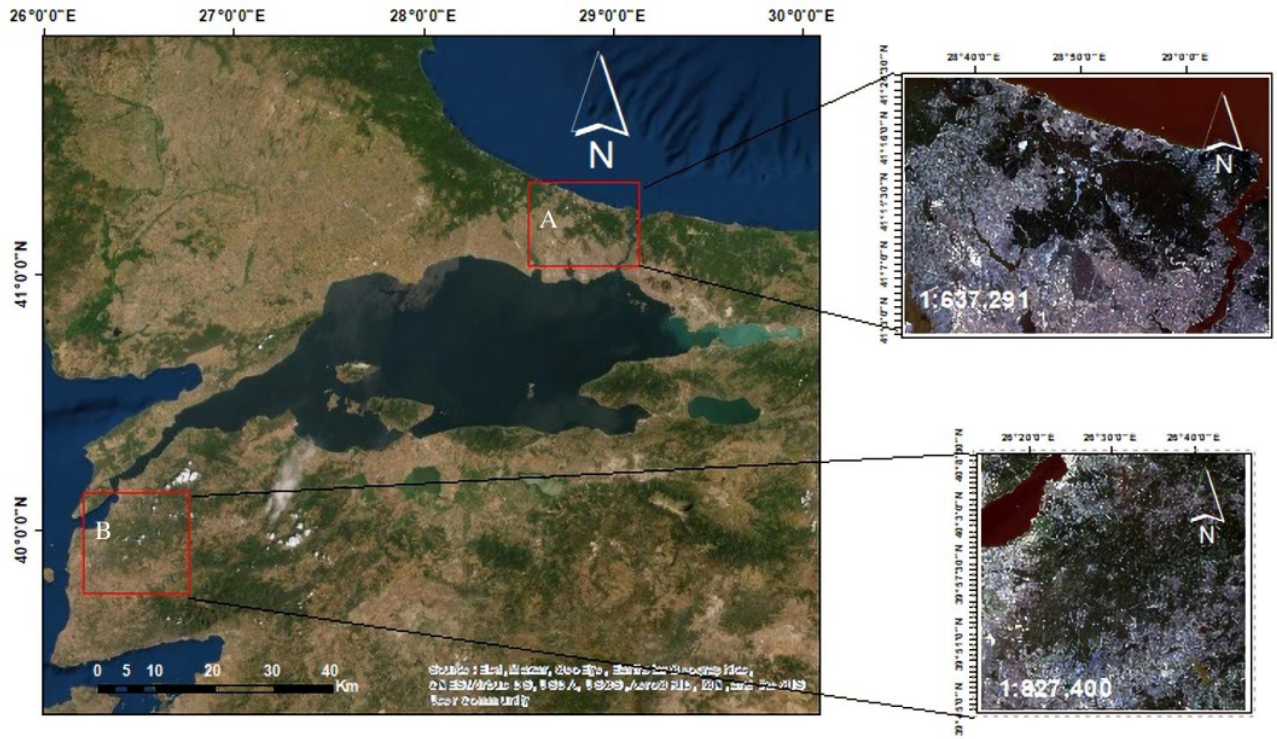

Figure 4.3 : Location of two study areas. A) Euxine–Colchic deciduous forests over Isanbul B) Anatolian conifer and deciduous forests over Çanakkale province.

Study area A : This site is located in the northern part of Istanbul city in the following coordinate, UTM 35 N WGS84, and extent of 4577505 m north and 678195 m east in Turkey. Istanbul with an approximately 5400 km^2 area is the largest city of Turkey with about 15,462,452 people. This city is known as not only a cultural and historical center but also known as an economical center of Turkey (Alganci, 2019). Istanbul located between the Black Sea and Marmara regions and takes advantages of different climatic conditions. This metropolitan city has warm and hot weather during the summer while winter is rainy and mild (Unal et al., 2011). It is indicated that the annual precipitation of Istanbul in the year 2020 was 820 mm and an average temperature of 14.95 ^oC. This study site has been selected due to the acceleration, in urban expansion, which led to deforestation and forest disturbances.

Study area B : The second study area is located in Çanakkale province, in northwestern Turkey with the coordinates of UTM 35N WGS84, 4443705 m north and 480555 m east. Çanakkale such as Istanbul has European and Asian parts with 541,548 people. It is located among the Aegean Sea, Çanakkale Strait, and the Marmara Sea. Its climate is characterized by hot and dry summer and cold, windy, and rainy winter (Kale, 2017).

The reason for selecting thiese two sites was the massive deforestation in Istanbul due to airport construction and the second one is deforestation in Çanakkale province because of mining activities. This study used BFASTspatial analysis to evaluate the accuracy of this method to detect the deforestation different from the other studies which used this algorithm to detect deforestation induced by fire (Hulley et al., 2014).

4.2 Data Acquisition and Preprocessing

From historical investigations, it is proved that the truthfulness of conducting time series analysis of satellite imagery highly depend upon the accuracy of image preprocessing and homogeneity of satellite images. These are divided to numerous steps, defined in the literature in the next steps.

4.2.1 Satellite data

In this study, Landsat 8 OLI, Collection 1 Level 2 satellite image products were used as the inputs. Level 2 processed Landsat 8 OLI image contains surface reflectance products that are geometrically and radiometrically corrected and quantized by 10000 scale factor. The Landsat satellite images have a 30-meter spatial resolution with 16-day temporal resolution. In Landsat 8 the sensor was updated to Operational Land Imager (OLI) and Thermal Infrared Sensor (TIRS), which together are contained eleven spectral bands and improved radiometric precision (USGS, 2019). Landsat Collection 1 Level 2 surface reflectance products are provided on-demand and in this respect, all of the images should be ordered from the personal account in Earth Explorer. The information about bands and wavelength is demonstrated in Table 4.1. Within the context of this study, all available Landsat 8 (OLI) data from two study areas (Path/Row, 180/031 and 181/032), that has cloud cover less than 10%, between the period of February 2013- December 2020 were ordered and downloaded. Overally 70 images that meet the criteria were used for this study.

Table 4.1 : Bands information of Landsat 8 OLI.

Bands	Wavelength (micrometer)	Resolution (meter)
Band 1 - Coastal aerosol	0.43-0.45	30
Band 2 - Blue	0.45-0.51	30
Band 3 - Green	0.53-0.59	30
Band 4 - Red	0.64-0.67	30
Band 5 - Near Infrared (NIR)	0.85-0.88	30
Band 6 - SWIR 1	1.57-1.65	30
Band 7 - SWIR 2	2.11-2.29	30
Band 8 - Panchromatic	0.50-0.68	15
Band 9 - Cirrus	1.36-1.38	30
Band 10 - Thermal Infrared (TIRS) 1	10.6-11.19	100
Band 11 - Thermal Infrared (TIRS) 2	11.50-12.51	100

4.2.2 Image preprocessing

As it is mentioned in above sections, the accuracy of time series analysis is highly related to the preprocessing steps. Fortunately, the Landsat 8 Collection 1 Level 2 surface reflectances product has already been geometrically and radiometrically corrected. The only remaining steps are cloud and cloud shadow masking and optionally using scale factor to put all bands in the range between 0-1, the scale factor for collection 1 data is 0.0001. Pixel QA is used to mask cloud and cloud shadow in R with the processLandsatBatch function. For the sake of purpose of this thesis, investigating deforestation, the forest mask of two study regions were performed to ensure only forested areas were observed and monitored for detecting changes according to follow:

The initial step, inspiring from the works of Schultz et al., (2013) and Sexton et al., (2013) was to create a forest mask over each of study area, with respect to the Landsat satellite image from the first year of this study which is the year 2013, without inclusion of any clouds and/or cloud shadows .

Landsat Vegetation Continuous Field (VCF) (Sexton et al., 2013) product, with criteria of canopy cover more than 30% and forest area at least 0.5 ha was selected as a base map for the Areas of Interest (AOI) in this thesis. As Landsat VCF was prepared with 5 years interval (e.g. 2005, 2010, 2015) the map for 2010 was selected to be updated for the year 2013. As Landsat images are including cloud and cloud shadows, in order to achieve full data coverage of forest areas, all images from the begnning of this study were used to update VCF map to achieve full data coverage of foreast areas. Initially, with respect to VCF map of 2010, the surface reflectance images from the beginning of study, 2013, were classified to the first canopy cover greater than 30% and then non-forest areas by using the supervised Random Forest classifier. To meet the second criteria, forest classes with an area less than 0.5 ha was considered as no class.

4.3 Vegetation indices

Generally, due to the complexities defining the proportion and magnitude of the single object change in a remotely sensed image and decompose it to recognizable parameters, index based approaches were determined and characterized (Bannari et al., 1995). In the context of remote sensing the irradiance and reflectance characteristic of the surface determine the amount and proportion of light that reflect from the

surface (Huete, 2014).Vegetation indices (VI), known as dimensionless quantitative radiometric measurements (Asrar et al., 1984) for characterizing the physical properties of vegetation. It should be considered that there is not a single standard value for vegetation indices and their value can be changed according to different research (Bannari et al., 1995). With the developments of these indices, scientists gained the chance to more effectively interpret satellite images, in comparison with just using individual spectral bands.

The main reason for developing plethora numbers of VIs is the fact that there are several numbers of variables that can affect the satellite based assessment of the light, reflected from the ground. Especially, in respect to vegetation measurements these factors can be listed such as, atmospheric conditions, geometric conditions, solar radiations, soil moisture, leaf geometry, chemistry, and morphology, vegetation type, and behavior, the density of canopy and vegetation land cover (Bannari et al., 1995; Hewison & Kuras, 2005). Reducing the effect of such factors myriad numbers of vegetation indices were developed to find the more robust one. These variety of VIs depend upon the availability of spectral bands in the satellite images (Huete, 2014).

VIs utilize different range of bands (usually two or more) in Electromagnetic Spectrum (EMS) to demonstrate different aspects of vegetation. VIs provide the opportunity to make a comparison between different vegetation types and simultaneously recognize any changes in vegetated areas. In general, healthy vegetation indicates high reflectance in Near Infrared (NIR) and absorption in the visible range of EMS.

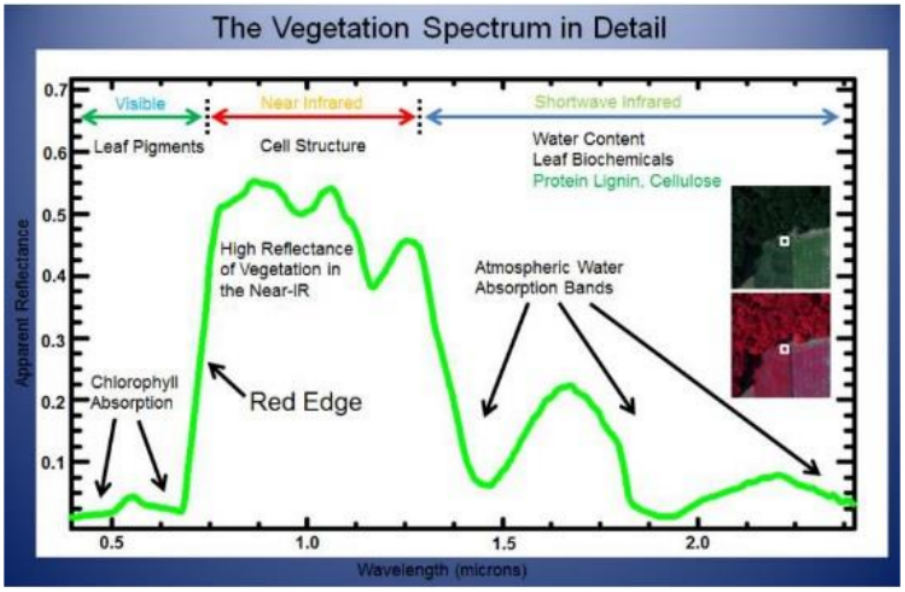

Figure 4.4 : Example of EM spectral signiture of healthy vegetation with absorption and reflectance.

There are several methods for characterizing forest dynamics with respect of time series analysis but it is proved that using spectral indices are pervaisive and indicates effective result (Hislop et al., 2018; Roy et al., 2014), due to sensitivity of spectral band to the forest land cover change (B DeVries, 2015). Spectral indices provide the ability to interpret the trajectory of every single pixels through the time series by converting the multi-spectral satellite image into a single component (Ben DeVries, Verbesselt, et al., 2015; Schultz, Clevers, et al., 2016). Furthermore, VIs by providing the combination of spectral bands enhances the spectral influence of green vegetation and canopy greenness to contribute volume and heath in different vegetation types (Hislop et al., 2018). The thematic characteristic of individual pixels of vegetation indices with different amounts of absorption and reflectance of solar radiation in disparate profiles with variation in canopy cover conditions has been shown in Figure 4.5.

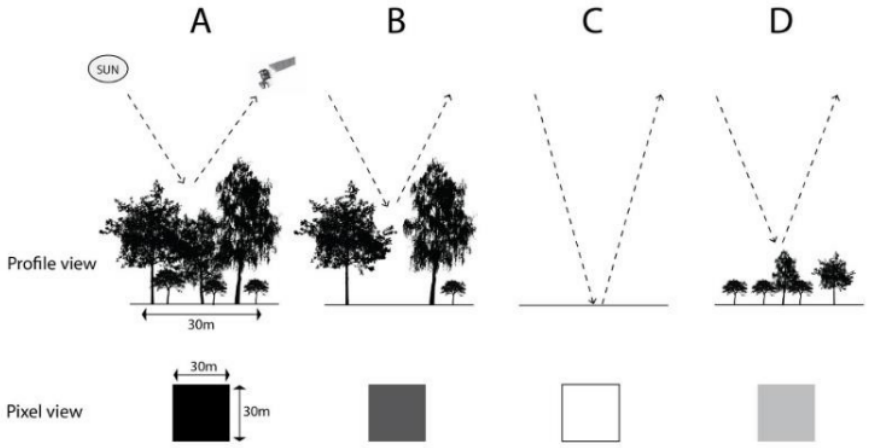

Figure 4.5 : Indication of forest canopy reflectance received by passive optical sensors. (A) complete forest, (B)degraded forest with canopy gap, (C) cleared forest, (D) regrowing forest. The bottom thematic of pixels illustrates the impact of different land surface and profile reflectance on a hypothetical vegetation index over 30-meter Landsat data pixels (B DeVries, 2015).

In this thesis, to evaluate performance of them through BFAST analysis in detecting deforestation a set of four vegetation indices have been selected. The detailed explanation of priorities and features related to these VIs is provided in the forward sections. According to the previous research in the context of using vegetation indices in time series analysis of deforestation it is proved that combination of SWIR and NIR in a spectral index lead to producing accurate results from BFAST analysis (Bueno et al., 2020a; Ben DeVries, Verbesselt, et al., 2015; Muñoz et al., 2020; Quevedo & Gao, 2017; Schultz, Clevers, et al., 2016; Smith et al., 2019; Jan Verbesselt et al., 2012a). In this regard, to make an accurate comparison the different VIs with different range of wavelengths in electromagnetic spectrum were selected.

4.3.1 Normalized Difference Vegetation Index (NDVI)

One of the most usable vegetation indices particularly to detect deforestation and forest degradation is the Normalized Difference Vegetation Index (NDVI). The chlorophyll in green vegetation and plants absorbs red lights during photosynthesis and scatter near-infrared wavelengths, because of the special structure inside the leaves. Therefore, high NDVI values indicate high-vegetated areas such as canopy closure, leaf biomass, and leaf area. The applicability of calculating NDVI from different

satellites, its advanced ability to monitoring vegetation, not only lead to considerable attention to this VI, but make it convenient for interpreting vegetation.

$$NDVI = \frac{\rho_{NIR} - \rho_{Red}}{\rho_{NIR} + \rho_{Red}} \quad (4.1)$$

The index values range between -1 to +1. The higher NDVI values are associated with healthy vegetation; inversely the lower NDVI values indicate either low vegetation or non-vegetation land surface.

4.3.2 Enhanced vegetation Index (EVI)

There are several number of studies; which proved that Enhanced Vegetation Index (EVI) is highly correlated with photosynthesis and plant transpiration. This VI not only has been markedly demonstrated sensitivity to red band but also variation in the blue band reflectance. While NDVI mostly responds for variation in the red band, EVI is responsive to NIR. Moreover, NDVI in the region with dense canopy cover or a high amount of Leaf Area Index (LAI) shows the saturation issue which is the other reason for developing EVI.

$$EVI = G * \left(\frac{(\rho_{NIR} - \rho_{Red})}{(\rho_{NIR} + C1 * \rho_{Red} - C2 * \rho_{Blue} + L)}\right) \quad (4.2)$$

4.3.3 Normalized Difference Moisture Index (NDMI)

Normalize Difference Moisture Index (NDMI) mostly is used to defined vegetation water content, water stress, and plant biomass changes, calculated by application of NIR and SWIR, in this regard it is sensitive to canopy cover and absorption by leaf moisture (Schultz, Clevers, et al., 2016), therefore it has the potential of detecting deforestation.

$$NDMI = \frac{\rho_{NIR} - \rho_{SWIR1}}{\rho_{NIR} + \rho_{SWIR1}} \quad (4.3)$$

4.3.4. Normalized Burn Ratio (NBR)

Recently Normalized Burn Ration (NBR) and its second version (NBR2) have been widely used in Landsat time series, due to their sensitivity to detect forest fires and burn severity; moreover, it is proven that in the context of characterizing forest dynamics, these spectral indices have considerable abilities for various forest areas.

$$NBR = \frac{\rho_{NIR} - \rho_{SWIR2}}{\rho_{NIR} + \rho_{SWIR2}} \quad (4.4)$$

Where:

NIR-Near-infrared (Band 5 in Landsat 8)

Red- Red band (Band 4 in Landsat 8)

Blue- Blue band (Band 2 in Landsat 8)

$SWIR_1$-Short-wave infrared 1 band (Band 6 in Landsat 8)

$SWIR_2$- Short-wave infrared 2 band (Band 7 in Landsat 8)

G – Gain factor for correction (2.5 for Landsat 8)

C1 & C2 – Coefficients of aerosol resistance term Blue (6&7.5 for Landsat 8 respectively)

4.4 Analysis Environment

Three main software has been used in this thesis, ArcGIS, Google Earth, R and Rstudio. R is open-source software that use for statistical programming language. Using R in combination with Rstudio is prevasive tool among researchers and data specialists to develop statistical programing as well as analyzing data. This software benefits from robust features such as numerous graphics and visualization tools, debugging and code editing. There are several numbers of packages for various usage, provided in R and being developed by different R communities such as the Comprehensive R Archive Network (CRAN). ArcGIS in this thesis was used to

analyze the out put from ‘bfastspatial’. ArcGIS is used for various purposes such as mapping and visualization, remote sensing imagery, and spatial analysis purposes.

Google Earth is a free powerful mapping platform, developed and released by Google in 2001. The main objective of using this p;atform in the thesis is to validate the accuracy of the output from ‘bfastspatial’ as well as near real time assessment as there is the time-lapse data in Google Earth which provides the ability to have access to the high spatial resolution imagery from different years.

4.5 Analysis Framework

To initialize the system to perform ‘bfastspatial’ algorithm there are some prior arrangements. In the first step pre-processed data, downloaded from USGS, was placed in the directory named landsat. All folder structure related to the algorithm is indicated in Figure 4.6. All of these directories also require to be created in R environment, to do so function command such as landsatDir <- file.path(stepDir, 'landsat') was used (see Appendix A for coding).

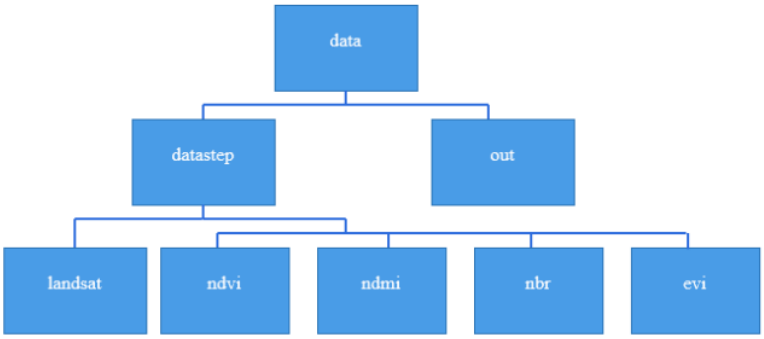

Figure 4.6 : Folder architecture that needs to be created outside of R environment on the computer.

Then the “processLandsatBatch” function which is part of ‘bfastspatial’ package, was used to calculate the vegetation indices from Landsat images. This function includes set of tools that meet the requirements of different projects. As an example “pixel_qa” is the tool to perform cloud masking of the images, “extent” tool is used to be sure all of the images have the same ectend according to the study area, and also “vi” tool enable defining the type of VI that will be calculated. The VI images produced by this

tool where stored in separate folders and then were used to create brick object types by utilizing the "timeStack" function, which is another function inside "bfastspatial" package. Each of the raster brick contains layers and these layers are the VI images from 2013 to 2020. These images stacked together to built a VI time series which was served as inputs for "bfmSpatial". Before running the "bfmSpatial" model the "bfmpixel" tool was applied to make sure that there is a break inside the raster brick of VI. Once the break is detected then VI raster brick can be run through "bfmSpatial". There are several parameters inside this function that should be considered. After getting Landsat scene ID, the sensor information is defined. The internal function of "bfmSpatial" is the "bfastmonitor" which iteratively runs over each pixel of the raster brick. The parameters of the function:

data= time-series raster brick

start= start of monitoring period, which is in this thesis 2015

formula= response ~ harmonic

order=1

history= 2013 in this thesis

type = "OLS-MOSUM"

h=0.25

end=10

level=0.05

According to the previous research by B DeVries,(2015) and Verbesselt et al., (2012a) it is demonstrated that using first-order harmonic model with an h value of 0.25 provided the most accurate result. The h=0.25 means that a 4-year window of data is considered in computing of "OLS-MOSUM" statistics. In other words, by this amount of "h-value" only one break could be detected in every 4 years.

The other parameter of "bfmSpatial" is a user-defined parameter named "monitoring period", which is the period that the user anticipate to detect break. In this thesis, period of 2015-2020 is considered as monitoring period. Additional parameters that should be defined to ensure the the model run, are listed below:

x = time-series raster brick

dates = NULL (set internally within bfastSpatial)

pptype = 'irregular' (temporal resolution of images)

mc.cores = 5 (optional parameter in parallel processing it is defined the number of cores of your system to be included for processing the "bfmSpatial")

sensor = c("OLI") – (it is the sesor, included in the study could also be "ETM+ SLC-on", "ETM+ SLC-off" for Landsat 7 ETM+)

After finishing the process all over the pixels of the images the output of "bfastmonitor" is produced as a raster brick object with three different layers, named breakpoint, magnitude, and error respectively. The breakpoint layer is essentially the time of breaks that detected for each pixel, while the magnitude, defines the median of the residuals through monitoring period, and error layer provides the value of "1" for pixels when the error has been detected or "NA" when the method triumphed (Jan Verbesselt et al., 2015).

Having better manipulation of output layers, there is a function, named "changeMonth" for separation of breakpoints by year and month, also to create a map to just representing the magnitude of breaking points.

For the sake of this research by using "plot" function different type of outputs from the layer could be produced. In addition in order to assess the accuracy of the break points detected by this algorithm the outputs layers converted to the GeoTif files by using "writeRaster" function in R. After getting outputs there is a possibility to define the threshold og changes, so just the negative values would be remained, indicated the deforested areas. The workflow of this thesis is shown in Figure 4.8 which all of this steps is indicated.

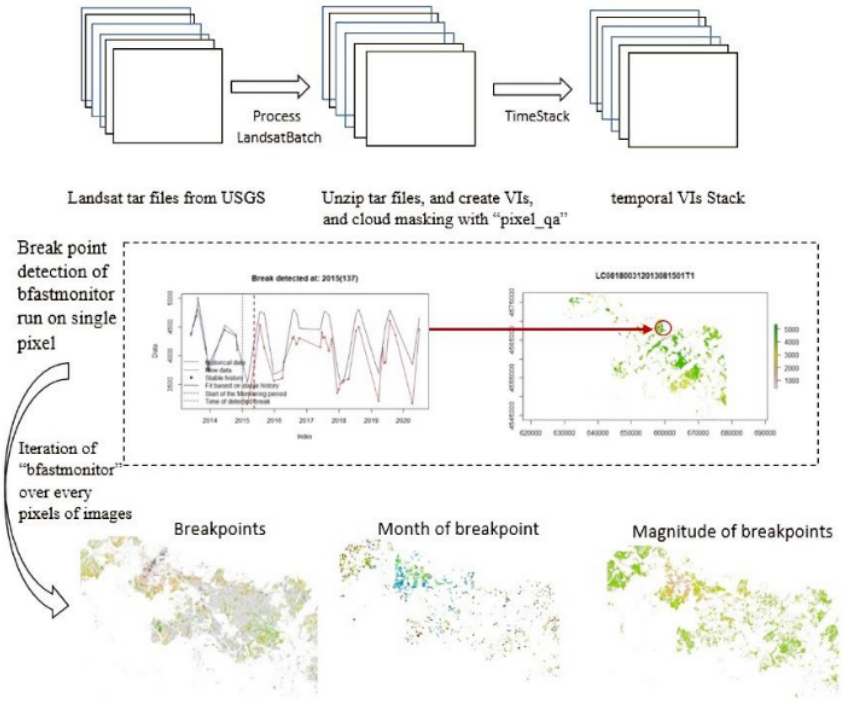

Figure 4.7 : Methodology diagram, applied to detect breakpoints in time series of landsat vegetation indices from 2015-2020 monitoring period. BFASTSpatial generates a map with the location of breakpoints labeled by date; a map of breakpoints per year labeled by a map of breakpoints per year labeled by month and a map of breakpoints labeled by change magnitude

4.6 Reference data and Accuracy Assessment

The main method of evaluating the BFAST to detect small-scale deforestation over both study areas was according to Congalton (1991) and Olofsson et al (2014), which broadly used in the concept of map validation in scientific studies. In this thesis the error matrix was used to compare map values, associated with the breakpoint magnitude from the BFAST, demonstrating of the deforestation, with the true ground data, provided from reference data, according to very high spatial resolution (VHR) satellite imagery by using Google Earth Pro software.

Using the error matrix there is the feasibility to calculate several mtrics of accuracy, including "Overall Accuracy (OA)", "Producer's Accuracy (PA)", "User's Accuracy (UA)", and "Bias". The OA is computed by the division of total number of correctly classified pixels by the total number of pixels in the error matrix. The PA refers to the ratio of total number of correct pixels in the category to the total number of pixels in that category based on the reference dataset. In fact, this accuracy is the probability of the number of reference data that are correctlyclassified, which also named as omission error. The UA is defined as the number of correctly classified pixels in a category divided to the total classified pixels in that category, known as commission error. Indeed, it is represented the probabiliity that a pixel that is classified in the image or map truly demonstrates that category in the ground. The "Bias" is measured by differencing between UA and PA.

For assessing the accuracy of the BFAST in the first stage by using ArcGIS stratified random points selecting according to the breakpoint magnitude of vegetation indices for each study area. For this purpose, 500 points for study area A and 700 points for study area B were selected. In the second stage these ground truth data were labeled according to whether they are representing of deforestation (D) or stable (S) land cover/ land use (Ben DeVries, Verbesselt, et al., 2015; Grogan et al., 2016; Murillo-Sandoval et al., 2017; Schultz, Clevers, et al., 2016; Smith et al., 2019). This information was extracted from multi-temporal very high spatial resolution (VHR) imagery by comparing the image of 2013 and end of 2020 through Google Earth platform. This platform provides Rapid Eye/ World View images with less than 5 meter spatial resolution for both test sites. During the monitoring period there were some regrowth areas, recognized from VHR by sufficient biomass. These areas were

picked up by BFAST as deforested areas (D). However, for validation purposes these areas are collected as stable (S) spots.

According to the previous studies B DeVries, (2015); Ben DeVries, Decuyper, et al., (2015) and Murillo-Sandoval et al. (2017) the threshold of change magnitudes <-0.05 for moderate to negative magnitude of "bfastspatial" for VIs was selected. The accuracy assessment was performed for all VIs (NDVI, NDMI, NBR, and EVI) and the accuracy ranks gained from them were compared together.

5. RESULT AND DISCUSSION

In this thesis, the accuracy of BFAST method in detecting small-scale deforestation in two different types of forests located in Turkey were evaluated. The important concern about this method was the availability of data as Landsat temporal resolution is every 16 days. Moreover, clouds and cloud shadows reduced the number of observed pixels in study areas due to masking them from images by image quality mask.

Overall, the "bfatspatial" algorithm indicated the great performance of processing time and accuracy results. Generally, the size of downloaded images for study area A was 14 GB and study area B about 23 GB. All of the processing was done on a computer system with windows 10, i7 core, 4GHz (8CPUs), 32GB RAM.

Time series raster brick creation was efficient and took a time about 5 minutes or less. However, running "bfmspatial" was the most time-consuming part of the process, with about 30-45 minutes to produce the output breakpoints, magnitude, error, and other supplementary outputs, which were around 23 MB for study area A and 153 MB for study area B.

5.1 Breakpoints and Magnitude

The distribution map of breakpoints during 2015-2020 for each site, is given in Figures 6.1 and 6.2. In these maps the breakpoints are labeled according to their magnitude values using a red > yellow > green color gradient scheme. Red color corresponds to slight to extreme negative breakpoint magnitudes, while yellow and green correspond to slight to moderate positive breakpoint magnitudes. In the study area A there is a higher amounts of breakpoints in comparison with site B. In the site A, the larger area of deforestation occured during the monitoring period which is from 2015-2020 belongs to the construction of the new airport in Istanbul. It is indicated that BFAST algorithm provides efficient results in detecting deforestation in this study area. In table 6.1 the percentage of breakpoints pixels which are detected by using BFAST algorithm, for each VI is shown. According to this table, around 13% of total

forest pixels of study area A, is detected as breakpoints by NDMI, while this varied to almost 22%, by utilizing EVI in the model. The map of magnitude of breakpoints in t site B, indicated in Figure 6.2. Conversely, in site B the percentage of pixels that is labeled as breakpoints according to Table 6.2 is changed from almost 3% by EVI to 7.4% by both NDVI and NBR.

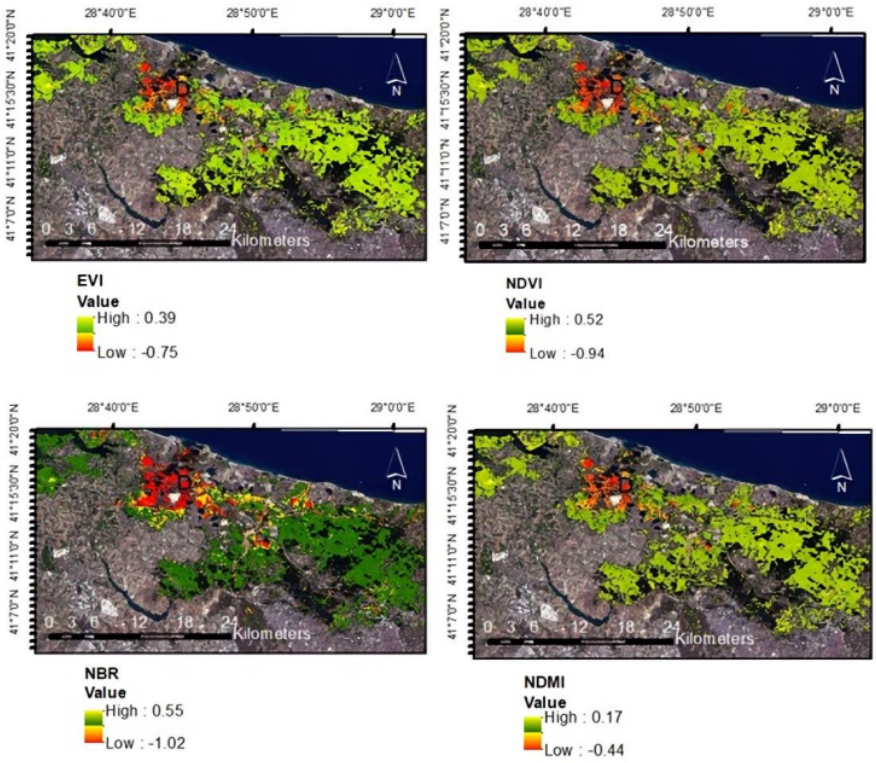

Figure 5.1 : Magnitude values for all detected breakpoints in study area A.

Table 5.1 : Pixel percentages of VIs for the study area A.

Vegetation Index	NDVI	NDMI	NBR	EVI
Breakpoint Pixels	45195	35515	49510	61679
Total Pixels	275913	275913	275913	275913
Percentage	16.38%	12.87%	17.94%	22.35%

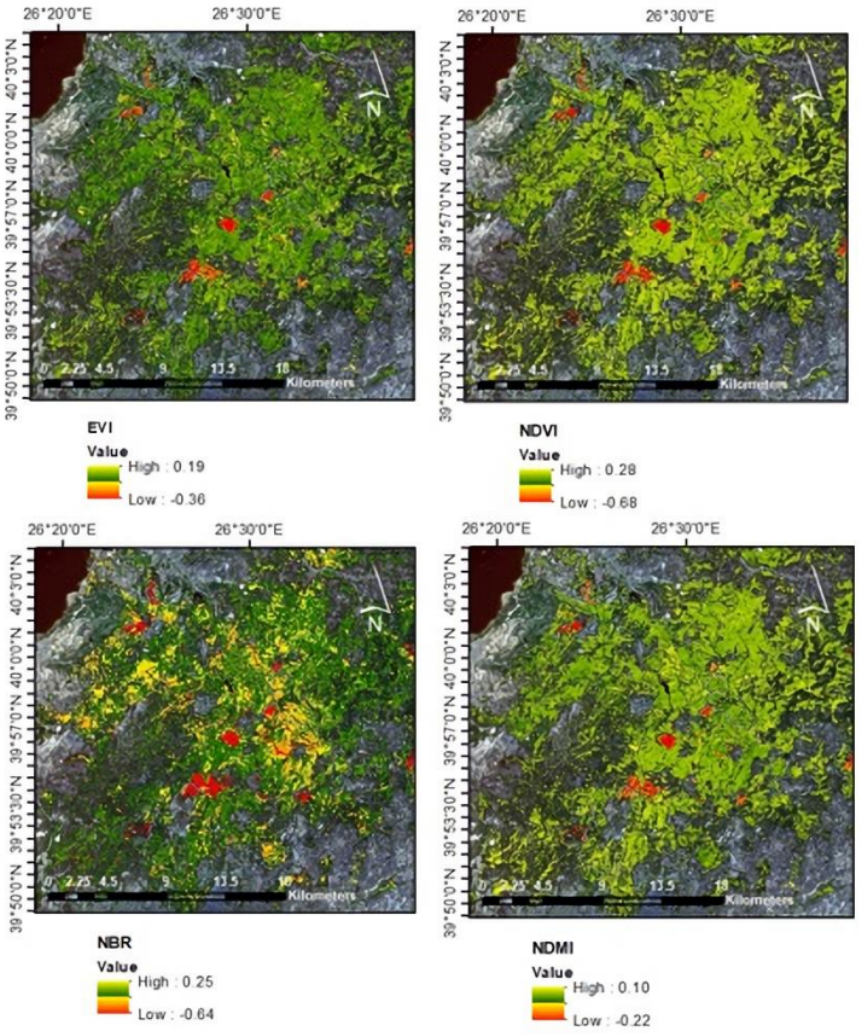

Figure 5.2 : Magnitude values for all detected breakpoints in study area B.

Table 5.2 : Pixel percentages of VIs for the study area B.

Vegetation Index	NDVI	NDMI	NBR	EVI
Breakpoint Pixels	24537	14243	34921	13239
Total Pixels	471281	471281	471281	471281
Percentage	5.20%	3.02%	7.40%	2.80%

Breakpoints magnitude was the most significant estimator of deforestation event with the most negative values, correlated most to the deforestation. The magnitude values was interestingly various in both different study areas and vegetation indices. In site A it is broadly change from extreme negative to extreme positive associate with EVI

from -1.02 to 0.55 while in site B extreme values change from -0.68 to 0.28 associated with NDVI.

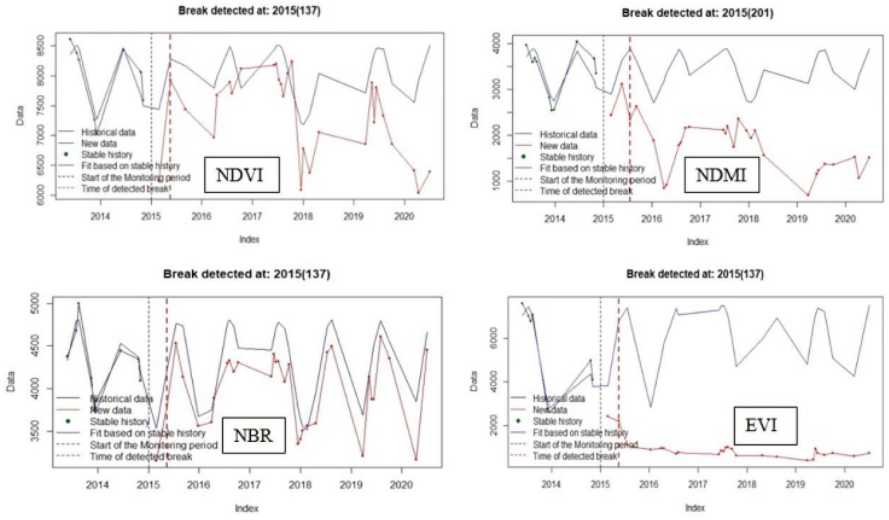

Figure 5.3 : Time series of break detection for all VIs over study area A according to"bfmpixel" function.

The time series of historical period and monitoring period according to the breakpoints for study area A and B with "bfmpixel" function is demonstrated in Figure 6.3 and Figure 6.4 respectively. The function "bfmpixel" was used to detect the break in the timeStack of vegetation indices from Landsat images. Time series of study area A represented the break in day 137 of the year 2015, while study area B demonstrated the break in day 32 of the year 2015. It is worth to mention that in site B the amount of variation in seasonalities due to the small areas of deforestation is shallow. While in site A seasonalty of time series is deeper because of large area of deforestation.

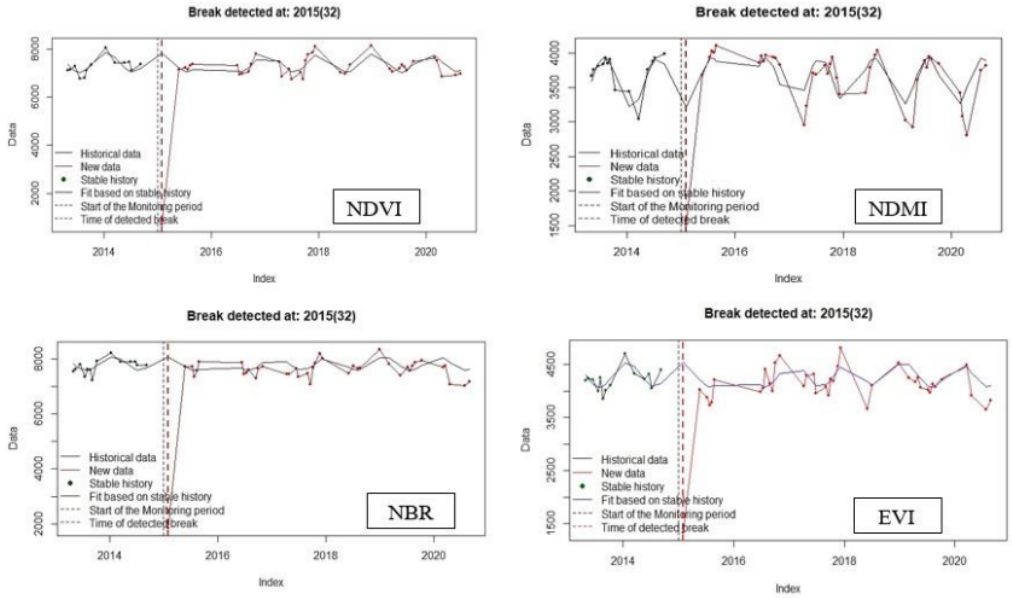

Figure 5.4 : Time series of break detection for all VIs over study area B according to "bfmpixel" function.

B DeVries, (2015) and Schultz, Clevers, et al., (2016) demonstrated that moderate to extreme negative values are associated with the decrease in forest cover. It is because the significant negative values only occures when there is the conversion in land cover from vegetated area to the other types of land cover. The yellow to green values represented extreme positive values of breaks, which considered the sudden increase in the values of the vegetated areas. One idea behind this could be increase in the amount of precipitation in the area which results in slight increment at VIs such as NBR and NDMI. In this thesis, the focus was on the moderate to extreme negative values, indicated deforestation in the study areas.

5.2 Accuracy Assessment

The overall accuracies of vegetation indices across study area A, proved that all vegetation indices (NDVI, NDMI, NBR, and EVI) indicated high accuracy by using BFAST method. However, the NDMI and NDVI provide comparatively lower accuracy in deforestation demonstration with OA around 85%. In general, overall accuracies of VIs for study area B were slightly higher than the accuracies for study area A, but interestingly in study area B, the NDMI and NDVI demonstrated the

highest accuracies by 88% and 89% respectively. For better visualization of accuracy assessment results, overall accuracies, user's accuracies, and producer's accuracies are represented in tables 6.3 to 6.10 for study areas A and B.

Table 5.3 : The accuracy assessment of NDVI for site A.

NDVI	D	S	Total	UA
D	101	14	115	87.82%
S	62	323	385	83.89%
Total	163	337	500	
PA	61.96%	95.84%	**OA=**	84.8%

Table 5.4 : The accuracy assessment of NDMI for site A.

NDMI	D	S	Total	UA
D	99	13	115	86.08%
S	64	324	385	84.15%
Total	163	337	500	
PA	60.73%	96.14%	**OA=**	84.6%

Table 5.5 : The accuracy assessment of NBR for site A.

NBR	D	S	Total	UA
D	103	19	122	84.42%
S	60	318	378	84.12%
Total	163	337	500	
PA	63.19%	94.36%	**OA=**	84.2%

Table 5.6 : The accuracy assessment of EVI for site A.

EVI	D	S	Total	UA
D	101	44	142	71.12%
S	62	293	355	82.53%
Total	163	337	500	
PA	61.96%	86.94%	**OA=**	78.8%

Table 5.7 : The accuracy assessment of NDVI for site B.

	D	S	Total	UA
D	126	10	136	92.64%
S	71	493	564	87.41%
Total	197	503	700	
PA	63.95%	98.01%	**OA=**	88.42%

Table 5.8 : The accuracy assessment of NDMI for site B.

	D	S	Total	UA
D	119	1	120	99.16%
S	78	502	580	86.55%
Total	197	503	700	
PA	60.40%	99.80%	**OA=**	88.71%

Table 5.9 : The accuracy assessment of NBR for site B.

	D	S	Total	UA
D	131	23	154	85.06%
S	66	480	546	87.91%
Total	197	503	700	
PA	66.49%	95.42%	**OA=**	87.28%

Table 5.10 : The accuracy assessment of EVI for site B.

	D	S	Total	UA
D	118	4	122	96.72%
S	79	499	578	86.33%
Total	197	503	700	
PA	59.89%	99.20%	**OA=**	88.14%

The values of producer's accuracies that represent the omision error for site A for all are approximately the same with about 1% difference for all VIs. In this site NDVI and NBR provided higher values of producer's accuracies with 62% and 63% respectively. Furthermore, in site B same as site A, NDVI and NBR provided higher accuracies with 64% and 66% . The user's accuracy represented the higher values for site B in comparison with site A as a result of the lower deforestation areas. This amount change from 70% to 88% in site A and 85% to 99% in site B.

To summarize, in this BFAST based deforestation analysis the NBR and NDMI provided more accurate results in comparison with EVI and NDVI especially for site A. It is proved that the vegetation indices which take advantage of SWIR and NIR bands are considerably more sensitive to the canopy moisture, thus provide more accurate deforestation detection espesifically in deforestation patches. On the other hand, the VIs that calculated with use of Red and NIR bands, demonstrated slightly less performance in comparison with NDMI and NBR. However, these differences are insignificant.

J. Verbesselt et al., (2006), proved that NDMI, demonstrated accurate result in herbaceous biomass in savanna ecosystems in fire risk detection due to SWIR

sensitivity to the water in plant tissue. In the other earlier studies such as Wilson & Sader (2002), the performance of NDVI and NDMI related to forest harvest type detection with use of Landsat imagery were investigated. They used the old method of comparing 2 images from different intervals. Their results showed that the NDMI in all intervals is considerbly outperforming NDVI in detecting clearcuts more specifically in small-scale harvested areas. In this thesis, it has been found that the vegetation indices related to water absorption portions of the electromagnetic spectrum such as NDMI and NBR are more sensitive to the changes of forest canopy compared to vegetation indices associated with the chlorophyll absorption, thus calculated with the Red and NIR bands such as NDVI and EVI. Sims and Gamon (2003), revealed that the ability of remote sensors to acquire information of a forest canopy is directly related to the strong absorption of wavelengths. In this regard, the vegetation indices such as NDVI, which has not the ability to deeply penetrate the forest canopy due to the absorption of chlorophyll especially throughout the leaves of the canopy, faces information loss.

Schultz et al. (2013) indicated that commission errors occured due to the uncorrected atmospheric effects, which in the context of BFAST is related to the cloud shadow and cloud cover. Bias is related to differences between omission and commission errors. If bias has the positive values it indicates that the errors from overestimation is higher than the errors from underestimation in evaluation while for negative values of bias the opposite would be true. In this thesis the amount of bias related to each VIs and for each study area represented in Figure 6.5. It is obvious from this figure that bias has a arised with the positive values, overestimation error has been occured. Overall, site A indicated lower bias than site B. More specifically in site A, EVI had the lowest amount with 9.6% of bias. Schultz, Clevers, et al (2016) proved that fusion of vegetation indices is the efficient method to reduce bias. In their study they tested each feasible combination of data fusion among VIs this is not in the context of this thesis but could be considered for a future investigation related to deforestation detection.

5.3 The Source of Error in Implementation of BFAST

There are several source of errors related to the BFAST algorithm, which were investigated by Schultz et al. (2013). In this thesis the primary source of error was lack of data due to the cloud shadow and cloud cover. Cloud cover is known as a significant source of error in the investigation of time series analysis with BFAST algorithm. This

effect was more significant in study area A the total number of pixels for the 48 images from 2013-2020 after forest masking were almost 18,195,552 and 13,243,824 of them remained after cloud masking, which means almost 27% of the input pixels were flagged as NA (Not Applicable).

Figure 5.5 : the percentage of bias against percentage of overall accuracy for site A and B. The positive values of bias represent that overestimation error was higher than underestimation.

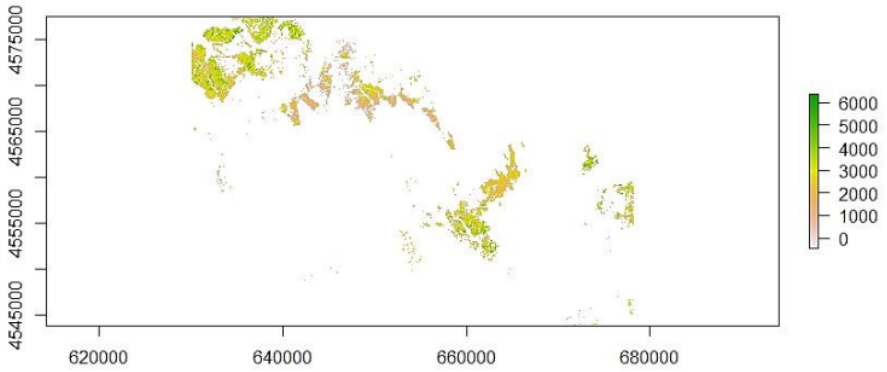

Figure 5.6 : 12.01.2016 dated image of study area A from EVIStack, showing lack of data.

5.4 Discussion

Forest resources play prominent role not only in supplying facilities and food for human being but also for survival of embryos and animals. Implementation and progress of such a technology to address the deforestation and forest degradation more specifically in the areas with scarce resources would be vitally important. With the use of BFAST algorithm and proper magnitude map from proper data, there is a feasibility to acquire probable deforestation, correlated to the lowest amount of magnitude class. Produced-probable deforestation map could be used as a reference to further investigation on the probable areas with several technologies such as drone monitoring or Terrestrial Laser Scanning (TLS) to prohibit of deforestation. Although the implementation of this map would require high-power computer systems, availability of data, stable internet connection, which means an increase for the need for financial support and sufficient budget. As a result it would not feasible without the collaboration of governments, stakeholders, universities, and organizations around the world.

6. CONCLUSION

Recently, the increasing rate of deforestation due to climate change and human-induced reasons performing investigating research that indicates methods and algorithms with high level of precisions and accuracies, play a prominent role to address this problem. Turkey includes different forest types with various species in them. Thus, it is essential to determine the method that works efficiently across different forest types and could help stakeholders and environmentalists to acquire information about the source of deforestation and statistical information related to this issue. As a result, this thesis investigated the performance of the BFAST set of algorithms in detecting deforested areas in two different sites of Marmara region in Turkey. This algorithm showed promising results in deforestation detection of tropical forest region and savanas in previous studies and in this study it is demonstrated that BFAST has the ability to detect deforestation in deciduous and conifer forests not only in large-scale deforested regions but also for small-scale deforested regions. More specifically in this thesis, it is validated that the parameters of BFAST defined in previous research can be used for different regions with high accuracy. Moreover, this thesis showed that the vegetation indices, which are more sensitive to the water in canopy forests with utilizing SWIR provided more accurate results in two study areas. It is worth to mention that in this thesis the most important source of error in implementing the BFAST algorithm was cloud covers, although Landsat images with less than 10% cloud covers were selected for this research. The impact of cloud cover is more essential when it is the reason for elimination of the pixels in the image whether it is included in historical period or monitoring period of BFAST algorithm, which is led to decreasing in the accuracy of the results. Overall, the BFAST set of algorithms represented promising and accurate results related to detecting deforestation by using Landsat image time series.

REFERENCES

Alganci, U. (2019). Dynamic land cover mapping of urbanized cities with landsat 8 multi-temporal images: Comparative evaluation of classification algorithms and dimension reduction methods. *ISPRS International Journal of Geo-Information*, *8*(3). https://doi.org/10.3390/ijgi8030139

Asner, G. P., Knapp, D. E., Broadbent, E. N., Oliveira, P. J. C., Keller, M., & Silva, J. N. (2005). Ecology: Selective logging in the Brazilian Amazon. *Science*, *310*(5747), 480–482. https://doi.org/10.1126/science.1118051

Asrar, G., Fuchs, M., Kanemasu, E. T., & Hatfield, J. L. (1984). Estimating Absorbed Photosynthetic Radiation and Leaf Area Index from Spectral Reflectance in Wheat 1 . *Agronomy Journal*, *76*(2), 300–306. https://doi.org/10.2134/agronj1984.00021962007600020029x

Atzberger, C. (2013). Advances in remote sensing of agriculture: Context description, existing operational monitoring systems and major information needs. *Remote Sensing*, *5*(2), 949–981. https://doi.org/10.3390/rs5020949

Bannari, A., Morin, D., Bonn, F., & Huete, A. R. (1995). A review of vegetation indices. *Remote Sensing Reviews*, *13*(1–2), 95–120. https://doi.org/10.1080/02757259509532298

Berberoğlu, S., Akin, A., & Clarke, K. C. (2016). Cellular automata modeling approaches to forecast urban growth for adana, Turkey: A comparative approach. *Landscape and Urban Planning*, *153*, 11–27. https://doi.org/10.1016/j.landurbplan.2016.04.017

Boriah, S. (2010). *Time series change detection: Algorithms for land cover change*. 160. http://adsabs.harvard.edu/abs/2010PhDT.....43B

Broich, M., Hansen, M. C., Potapov, P., Adusei, B., Lindquist, E., & Stehman, S. V. (2011). Time-series analysis of multi-resolution optical imagery for quantifying forest cover loss in Sumatra and Kalimantan, Indonesia. *International Journal of Applied Earth Observation and Geoinformation*, *13*(2), 277–291. https://doi.org/10.1016/j.jag.2010.11.004

Brooks, E. B., Wynne, R. H., Thomas, V. A., Blinn, C. E., & Coulston, J. W. (2014). On-the-fly massively multitemporal change detection using statistical quality control charts and landsat data. *IEEE Transactions on Geoscience and Remote Sensing*, *52*(6), 3316–3332. https://doi.org/10.1109/TGRS.2013.2272545

Bruzzone, L., Cossu, R., & Vernazza, G. (2004). Detection of land-cover transitions by combining multidate classifiers. *Pattern Recognition Letters*,

25(13), 1491–1500. https://doi.org/10.1016/j.patrec.2004.06.002

Bueno, I. T., McDermid, G. J., Silveira, E. M. O., Hird, J. N., Domingos, B. I., & Acerbi Júnior, F. W. (2020a). Spatial agreement among vegetation disturbance maps in tropical domains using Landsat time series. *Remote Sensing*, *12*(18). https://doi.org/10.3390/RS12182948

Bueno, I. T., McDermid, G. J., Silveira, E. M. O., Hird, J. N., Domingos, B. I., & Acerbi Júnior, F. W. (2020b). Spatial agreement among vegetation disturbance maps in tropical domains using Landsat time series. *Remote Sensing*, *12*(18). https://doi.org/10.3390/RS12182948

Bullock, E. L., Woodcock, C. E., & Olofsson, P. (2020). Monitoring tropical forest degradation using spectral unmixing and Landsat time series analysis. *Remote Sensing of Environment*, *238*(April), 0–1. https://doi.org/10.1016/j.rse.2018.11.011

Cai, X., Feng, L., Hou, X., & Chen, X. (2016). Remote Sensing of the Water Storage Dynamics of Large Lakes and Reservoirs in the Yangtze River Basin from 2000 to 2014. *Scientific Reports*, *6*(October), 1–9. https://doi.org/10.1038/srep36405

Chandra, P. (2011). Performance evaluation of vegetation indices using remotely sensed data. *International Journal of Geomatrics and Geoscience*, *2*(1), 231–240.

Chatfield, C., Crc, H., Crc, H., Zidek, J., Columbia, B., Smith, P. J., Bartholomew, D. J., Steele, F., Moustaki, I., Galbraith, J., Chatfield, C., Carlin, B. P., & Louis, T. A. (n.d.). *The Analysis of Time Series*.

Che, X., Feng, M., Yang, Y., Xiao, T., Huang, S., Xiang, Y., & Chen, Z. (2017). Mapping extent dynamics of small lakes using downscaling MODIS surface reflectance. *Remote Sensing*, *9*(1). https://doi.org/10.3390/rs9010082

Chen, J., Chen, X., Cui, X., & Chen, J. (2011). Change vector analysis in posterior probability space: A new method for land cover change detection. *IEEE Geoscience and Remote Sensing Letters*, *8*(2), 317–321. https://doi.org/10.1109/LGRS.2010.2068537

Chen, L., Michishita, R., & Xu, B. (2014). Abrupt spatiotemporal land and water changes and their potential drivers in Poyang Lake, 2000-2012. *ISPRS Journal of Photogrammetry and Remote Sensing*, *98*, 85–93. https://doi.org/10.1016/j.isprsjprs.2014.09.014

Cohen, W. B., Healey, S. P., Yang, Z., Stehman, S. V., Brewer, C. K., Brooks, E. B., Gorelick, N., Huang, C., Hughes, M. J., Kennedy, R. E., Loveland, T. R., Moisen, G. G., Schroeder, T. A., Vogelmann, J. E., Woodcock, C. E., Yang, L., & Zhu, Z. (2017). How Similar Are Forest Disturbance Maps Derived from Different Landsat Time Series Algorithms? *Forests*, *8*(4), 1–19. https://doi.org/10.3390/f8040098

Çolak, A. H., Rotherham, I. D., & Ian, D. (2011). A Review of the Forest

Vegetation of Turkey : Its Status Past and Present and a Review of the Vegetation Past and of Turkey : Present Its Status and Its Future. *Biology and Environment: Proceedings of the Royal Irish Academy*, *106*(3), 343–354.

Collins, L., Griffioen, P., Newell, G., & Mellor, A. (2018). The utility of Random Forests for wildfire severity mapping. *Remote Sensing of Environment*, *216*(June), 374–384. https://doi.org/10.1016/j.rse.2018.07.005

Congalton, R. G. (1991). A review of assessing the accuracy of classifications of remotely sensed data. *Remote Sensing of Environment*, *37*(1), 35–46. https://doi.org/10.1016/0034-4257(91)90048-B

Coppin, P., Jonckheere, I., Nackaerts, K., Muys, B., & Lambin, E. (2004). Digital change detection methods in ecosystem monitoring: A review. *International Journal of Remote Sensing*, *25*(9), 1565–1596. https://doi.org/10.1080/0143116031000101675

de By, R. A., Ellis, M. C., Georgiadou, Y., Kainz, W., Knippers, R. A., Kraak, M., Radwan, M. M., Sides, E. J., Sun, Y., Weir, M. J. C., & van Westen, C. J. (2001). *Principles of Geographic Information Systems - An introductory textbook*. 490.

DeFries, R., Achard, F., Brown, S., Herold, M., Murdiyarso, D., Schlamadinger, B., & de Souza, C. (2007). Earth observations for estimating greenhouse gas emissions from deforestation in developing countries. *Environmental Science and Policy*, *10*(4), 385–394. https://doi.org/10.1016/j.envsci.2007.01.010

Detsch, F., Otte, I., Appelhans, T., Hemp, A., & Nauss, T. (2016). Seasonal and long-term vegetation dynamics from 1-km GIMMS-based NDVI time series at Mt. Kilimanjaro, Tanzania. *Remote Sensing of Environment*, *178*, 70–83. https://doi.org/10.1016/j.rse.2016.03.007

DeVries, B. (2015). Monitoring tropical forest dynamics using Landsat time series and community-based data. In *Monitoring tropical forest dynamics using Landsat time series and community-based data* (Issue October 2016). https://pdfs.semanticscholar.org/015e/6ea68da0d181991d36ec7978b93c1391957c.pdf

DeVries, Ben, Decuyper, M., Verbesselt, J., Zeileis, A., Herold, M., & Joseph, S. (2015). Tracking disturbance-regrowth dynamics in tropical forests using structural change detection and Landsat time series. *Remote Sensing of Environment*, *169*, 320–334. https://doi.org/10.1016/j.rse.2015.08.020

DeVries, Ben, Verbesselt, J., Kooistra, L., & Herold, M. (2015). Robust monitoring of small-scale forest disturbances in a tropical montane forest using Landsat time series. *Remote Sensing of Environment*, *161*, 107–121. https://doi.org/10.1016/j.rse.2015.02.012

Dutrieux, Loïc P., Jakovac, C. C., Latifah, S. H., & Kooistra, L. (2016). Reconstructing land use history from Landsat time-series: Case study of a swidden agriculture system in Brazil. *International Journal of Applied Earth Observation and Geoinformation*, *47*, 112–124.

https://doi.org/10.1016/j.jag.2015.11.018

Dutrieux, Loïc Paul, Verbesselt, J., Kooistra, L., & Herold, M. (2015). Monitoring forest cover loss using multiple data streams, a case study of a tropical dry forest in Bolivia. *ISPRS Journal of Photogrammetry and Remote Sensing*, *107*, 112–125. https://doi.org/10.1016/j.isprsjprs.2015.03.015

Elburz, Z., çubukçu, K. M., & Nijkamp, P. (2018). The mutual relationship between regional income and deforestation: A study on Turkey. *Metu Journal of the Faculty of Architecture*, *35*(2), 77–87. https://doi.org/10.4305/METU.JFA.2018.2.4

Global Forest Resources Assessment 2015 Desk reference. (2015).

Grecchi, R. C., Beuchle, R., Shimabukuro, Y. E., Aragão, L. E. O. C., Arai, E., Simonetti, D., & Achard, F. (2017). An integrated remote sensing and GIS approach for monitoring areas affected by selective logging: A case study in northern Mato Grosso, Brazilian Amazon. *International Journal of Applied Earth Observation and Geoinformation*, *61*(April), 70–80. https://doi.org/10.1016/j.jag.2017.05.001

Griffiths, P., Kuemmerle, T., Kennedy, R. E., Abrudan, I. V., Knorn, J., & Hostert, P. (2012). Using annual time-series of Landsat images to assess the effects of forest restitution in post-socialist Romania. *Remote Sensing of Environment*, *118*, 199–214. https://doi.org/10.1016/j.rse.2011.11.006

Grogan, K., Pflugmacher, D., Hostert, P., Verbesselt, J., & Fensholt, R. (2016). Mapping clearances in tropical dry forests using breakpoints, trend, and seasonal components from modis time series: Does forest type matter? *Remote Sensing*, *8*(8). https://doi.org/10.3390/rs8080657

Hamunyela, E., Rosca, S., Mirt, A., Engle, E., Herold, M., Gieseke, F., & Verbesselt, J. (2020). Implementation of BFASTmonitor Algorithm on Google Earth Engine to support large-area and sub-annual change monitoring using earth observation data. *Remote Sensing*, *12*(18). https://doi.org/10.3390/RS12182953

Hansen, M. C., & Loveland, T. R. (2012). A review of large area monitoring of land cover change using Landsat data. *Remote Sensing of Environment*, *122*, 66–74. https://doi.org/10.1016/j.rse.2011.08.024

Hewison, D., & Kuras, M. (2005). Book reviews: Book reviews. *Journal of Analytical Psychology*, *50*(3), 395–403. https://doi.org/10.1111/j.0021-8774.2005.00541.x

Hislop, S., Jones, S., Soto-Berelov, M., Skidmore, A., Haywood, A., & Nguyen, T. H. (2018). Using landsat spectral indices in time-series to assess wildfire disturbance and recovery. *Remote Sensing*, *10*(3), 1–17. https://doi.org/10.3390/rs10030460

Huang, C., Goward, S. N., Masek, J. G., Thomas, N., Zhu, Z., & Vogelmann, J. E. (2010). An automated approach for reconstructing recent forest disturbance

history using dense Landsat time series stacks. *Remote Sensing of Environment*, *114*(1), 183–198. https://doi.org/10.1016/j.rse.2009.08.017

Huete, A. (2014). Vegetation indices. *Encyclopedia of Earth Sciences Series*, 883–886. https://doi.org/10.1007/978-0-387-36699-9_187

Hulley, G., Veraverbeke, S., & Hook, S. (2014). Thermal-based techniques for land cover change detection using a new dynamic MODIS multispectral emissivity product (MOD21). *Remote Sensing of Environment*, *140*, 755–765. https://doi.org/10.1016/j.rse.2013.10.014

Hüttich, C., Stelmaszczuk-Górska, M. A., Eberle, J., Kotzerke, P., & Schmullius, C. (2014). Operational Forest Monitoring in Siberia Using Multi-Source Earth Observation Data. *Сибирский Лесной Журнал*, *5*, 38–52. http://сибирскийлеснойжурнал.рф/upload/iblock/b21/b218d2553cc18c6379a15dfa4770d6f8.pdf

Irons, J. R., Dwyer, J. L., & Barsi, J. A. (2012). The next Landsat satellite: The Landsat Data Continuity Mission. *Remote Sensing of Environment*, *122*, 11–21. https://doi.org/10.1016/j.rse.2011.08.026

Jamali, S., Jönsson, P., Eklundh, L., Ardö, J., & Seaquist, J. (2015). Detecting changes in vegetation trends using time series segmentation. *Remote Sensing of Environment*, *156*, 182–195. https://doi.org/10.1016/j.rse.2014.09.010

Kale, S. (2017). Climatic Trends in the Temperature of Çanakkale City, Turkey. *Natural and Engineering Sciences*, *2*(3), 14–27. https://doi.org/10.28978/nesciences.348449

Kennedy, R. E., Yang, Z., & Cohen, W. B. (2010). Detecting trends in forest disturbance and recovery using yearly Landsat time series: 1. LandTrendr - Temporal segmentation algorithms. *Remote Sensing of Environment*, *114*(12), 2897–2910. https://doi.org/10.1016/j.rse.2010.07.008

Key, R. M., Kozyr, A., Sabine, C. L., Lee, K., Wanninkhof, R., Bullister, J. L., Feely, R. A., Millero, F. J., Mordy, C., & Peng, T. H. (2004). A global ocean carbon climatology: Results from Global Data Analysis Project (GLODAP). *Global Biogeochemical Cycles*, *18*(4), 1–23. https://doi.org/10.1029/2004GB002247

Lambert, J., Denux, J. P., Verbesselt, J., Balent, G., & Cheret, V. (2015). Detecting clear-cuts and decreases in forest vitality using MODIS NDVI time series. *Remote Sensing*, *7*(4), 3588–3612. https://doi.org/10.3390/rs70403588

Lambert, J., Drenou, C., Denux, J. P., Balent, G., & Cheret, V. (2013). Monitoring forest decline through remote sensing time series analysis. *GIScience and Remote Sensing*, *50*(4), 437–457. https://doi.org/10.1080/15481603.2013.820070

Langner, A. J. (2009). Monitoring Tropical Forest Degradation and Deforestation in Borneo, Southeast Asia. *GeoBio Center*, 176. https://edoc.ub.uni-muenchen.de/9953/1/Langner_Andreas.pdf

Liu, H., Zhang, Y., & Zhang, X. (2018). Monitoring vegetation coverage in tongren from 2000 to 2016 based on landsat7 etm+ and landsat8. *Anais Da Academia Brasileira de Ciencias*, *90*(3), 2721–2730. https://doi.org/10.1590/0001-3765201820170737

Loveland, T. R., & Dwyer, J. L. (2012). Landsat: Building a strong future. *Remote Sensing of Environment*, *122*(October 2000), 22–29. https://doi.org/10.1016/j.rse.2011.09.022

Lu, D., Mausel, P., Brondízio, E., & Moran, E. (2004). Change detection techniques. *International Journal of Remote Sensing*, *25*(12), 2365–2401. https://doi.org/10.1080/0143116031000139863

Lu, M., Hamunyela, E., Verbesselt, J., & Pebesma, E. (2017). Dimension reduction of multi-spectral satellite image time series to improve deforestation monitoring. *Remote Sensing*, *9*(10). https://doi.org/10.3390/rs9101025

Lu, M., Pebesma, E., Sanchez, A., & Verbesselt, J. (2016). Spatio-temporal change detection from multidimensional arrays: Detecting deforestation from MODIS time series. *ISPRS Journal of Photogrammetry and Remote Sensing*, *117*, 227–236. https://doi.org/10.1016/j.isprsjprs.2016.03.007

Lund, H. G. (2013). What Is A forest? Definitions Do Make A Difference An Example From Turkey. *AvrasyaTeriDergisi*, *2*(1), 1-8–8.

Mardian, J. (2020). *Evaluating the Utility of Remote Sensing Time Series Analysis for the Identification of Grassland Conversions in Alberta , Canada by ABSTRACT EVALUATING THE UTILITY OF REMOTE SENSING TIME SERIES ANALYSIS FOR THE IDENTIFICATION OF GRASSLAND*.

Mas, J. F. (1999). Monitoring land-cover changes: A comparison of change detection techniques. *International Journal of Remote Sensing*, *20*(1), 139–152. https://doi.org/10.1080/014311699213659

Matthews, J. A. (2014). Land-Change Science. In *Encyclopedia of Environmental Change*. https://doi.org/10.4135/9781446247501.n2200

Maxwell, S. K., Schmidt, G. L., & Storey, J. C. (2007). A multi-scale segmentation approach to filling gaps in Landsat ETM+ SLC-off images. *International Journal of Remote Sensing*, *28*(23), 5339–5356. https://doi.org/10.1080/01431160601034902

McKinney, M. L., & Lockwood, J. L. (1999). Biotic homogenization: A few winners replacing many losers in the next mass extinction. *Trends in Ecology and Evolution*, *14*(11), 450–453. https://doi.org/10.1016/S0169-5347(99)01679-1

Monitoring Structural Changes with the Generalized Fluctuation Test Author (s): Friedrich Leisch , Kurt Hornik and Chung-Ming Kuan Published by : Cambridge University Press Stable URL : https://www.jstor.org/stable/3533257 MONITORING STRUCTURAL CHANGES . (2000). *16*(6), 835–854.

Muñoz, E., Zozaya, A., & Lindquist, E. (2020). *Satellite Remote Sensing of Forest Degradation Using NDFI and the BFAST Algorithm*.

Murillo-Sandoval, P. J., Hoek, J. Van Den, & Hilker, T. (2017). Leveraging multi-sensor time series datasets to map short- and long-term tropical forest disturbances in the Colombian Andes. *Remote Sensing*, *9*(2), 1–17. https://doi.org/10.3390/rs9020179

Olofsson, P., Foody, G. M., Herold, M., Stehman, S. V., Woodcock, C. E., & Wulder, M. A. (2014). Good practices for estimating area and assessing accuracy of land change. *Remote Sensing of Environment*, *148*, 42–57. https://doi.org/10.1016/j.rse.2014.02.015

Pastick, N. J., Wylie, B. K., & Wu, Z. (2018). Spatiotemporal analysis of Landsat-8 and Sentinel-2 data to support monitoring of dryland ecosystems. *Remote Sensing*, *10*(5), 1–15. https://doi.org/10.3390/rs10050791

Peng, D., Hu, Y., & Li, Z. (2016). Spectral reflectance and vegetation index changes in deciduous forest foliage following tree removal: Potential for deforestation monitoring. *Journal of Applied Spectroscopy*, *83*(2), 330–337. https://doi.org/10.1007/s10812-016-0291-4

Pflugmacher, D., Cohen, W. B., Kennedy, R. E., & Yang, Z. (2014). Using Landsat-derived disturbance and recovery history and lidar to map forest biomass dynamics. *Remote Sensing of Environment*, *151*, 124–137. https://doi.org/10.1016/j.rse.2013.05.033

Platt, R. V., Ogra, M. V., Badola, R., & Hussain, S. A. (2016). Conservation-induced resettlement as a driver of land cover change in India: An object-based trend analysis. *Applied Geography*, *69*, 75–86. https://doi.org/10.1016/j.apgeog.2016.02.006

Portillo-Quintero, C., Sanchez-Azofeifa, A., Calvo-Alvarado, J., Quesada, M., & do Espirito Santo, M. M. (2015). The role of tropical dry forests for biodiversity, carbon and water conservation in the neotropics: lessons learned and opportunities for its sustainable management. *Regional Environmental Change*, *15*(6), 1039–1049. https://doi.org/10.1007/s10113-014-0689-6

Potter, C. (2019). Changes in Vegetation Cover of Yellowstone National Park Estimated from MODIS Greenness Trends, 2000 to 2018. *Remote Sensing in Earth Systems Sciences*, *2*(2–3), 147–160. https://doi.org/10.1007/s41976-019-00019-5

Purkis, S. J., & Klemas, V. V. (2013). Remote Sensing and Global Environmental Change. *Remote Sensing and Global Environmental Change*, *1995*, 1–367. https://doi.org/10.1002/9781118687659

Quevedo, A., & Gao, Y. (2017). Detection of forest disturbances by time series analysis of NDVI from MODIS sensor for Michoacan State, Mexico (2000 - 2014). *38th Asian Conference on Remote Sensing - Space Applications: Touching Human Lives, ACRS 2017*, *2017-Octob*(October).

Reiche, J., Verbesselt, J., Hoekman, D., & Herold, M. (2015). Fusing Landsat and SAR time series to detect deforestation in the tropics. *Remote Sensing of Environment*, *156*, 276–293. https://doi.org/10.1016/j.rse.2014.10.001

Romero-Sanchez, M. E., & Ponce-Hernandez, R. (2017). Assessing and monitoring forest degradation in a deciduous tropical forest in Mexico via remote sensing indicators. *Forests*, *8*(9). https://doi.org/10.3390/f8090302

Roy, D. P., Wulder, M. A., Loveland, T. R., C.E., W., Allen, R. G., Anderson, M. C., Helder, D., Irons, J. R., Johnson, D. M., Kennedy, R., Scambos, T. A., Schaaf, C. B., Schott, J. R., Sheng, Y., Vermote, E. F., Belward, A. S., Bindschadler, R., Cohen, W. B., Gao, F., … Zhu, Z. (2014). Landsat-8: Science and product vision for terrestrial global change research. *Remote Sensing of Environment*, *145*, 154–172. https://doi.org/10.1016/j.rse.2014.02.001

Saxena, R., Watson, L. T., Wynne, R. H., Brooks, E. B., Thomas, V. A., Zhiqiang, Y., & Kennedy, R. E. (2018). Towards a polyalgorithm for land use change detection. *ISPRS Journal of Photogrammetry and Remote Sensing*, *144*, 217–234. https://doi.org/10.1016/j.isprsjprs.2018.07.002

Schmidt, M., Lucas, R., Bunting, P., Verbesselt, J., & Armston, J. (2015). Multi-resolution time series imagery for forest disturbance and regrowth monitoring in Queensland, Australia. *Remote Sensing of Environment*, *158*, 156–168. https://doi.org/10.1016/j.rse.2014.11.015

Schultz, M. (n.d.). *Tropical deforestation monitoring using Landsat time series and breakpoint detection*.

Schultz, M., Clevers, J. G. P. W., Carter, S., Verbesselt, J., Avitabile, V., Quang, H. V., & Herold, M. (2016). Performance of vegetation indices from Landsat time series in deforestation monitoring. *International Journal of Applied Earth Observation and Geoinformation*, *52*(May 2012), 318–327. https://doi.org/10.1016/j.jag.2016.06.020

Schultz, M., Verbesselt, J., Avitabile, V., Souza, C., & Herold, M. (2016). Error Sources in Deforestation Detection Using BFAST Monitor on Landsat Time Series Across Three Tropical Sites. *IEEE Journal of Selected Topics in Applied Earth Observations and Remote Sensing*, *9*(8), 3667–3679. https://doi.org/10.1109/JSTARS.2015.2477473

Schultz, M., Verbesselt, J., Herold, M., & Avitabile, V. (2013). Assessing error sources for Landsat time series analysis for tropical test sites in Viet Nam and Ethiopia. *Earth Resources and Environmental Remote Sensing/GIS Applications IV*, *8893*(October 2013), 88930M. https://doi.org/10.1117/12.2029374

Sexton, J. O., Song, X. P., Feng, M., Noojipady, P., Anand, A., Huang, C., Kim, D. H., Collins, K. M., Channan, S., DiMiceli, C., & Townshend, J. R. (2013). Global, 30-m resolution continuous fields of tree cover: Landsat-based rescaling of MODIS vegetation continuous fields with lidar-based estimates of error. *International Journal of Digital Earth*, *6*(5), 427–448.

https://doi.org/10.1080/17538947.2013.786146

Sims, D. A., & Gamon, J. A. (2003). Estimation of vegetation water content and photosynthetic tissue area from spectral reflectance: A comparison of indices based on liquid water and chlorophyll absorption features. *Remote Sensing of Environment*, *84*(4), 526–537. https://doi.org/10.1016/S0034-4257(02)00151-7

Singh, A. (1989). Review Articlel: Digital change detection techniques using remotely-sensed data. *International Journal of Remote Sensing*, *10*(6), 989–1003. https://doi.org/10.1080/01431168908903939

Smith, V., Portillo-Quintero, C., Sanchez-Azofeifa, A., & Hernandez-Stefanoni, J. L. (2019). Assessing the accuracy of detected breaks in Landsat time series as predictors of small scale deforestation in tropical dry forests of Mexico and Costa Rica. *Remote Sensing of Environment*, *221*(May 2018), 707–721. https://doi.org/10.1016/j.rse.2018.12.020

Tran, B. N., Tanase, M. A., Bennett, L. T., & Aponte, C. (2018). Evaluation of spectral indices for assessing fire severity in Australian temperate forests. *Remote Sensing*, *10*(11). https://doi.org/10.3390/rs10111680

Trejo, I., & Dirzo, R. (2000). Deforestation of seasonally dry tropical forest: A national and local analysis in Mexico. *Biological Conservation*, *94*(2), 133–142. https://doi.org/10.1016/S0006-3207(99)00188-3

Tsutsumida, N., Saizen, I., Matsuoka, M., & Ishii, R. (2013). Land cover change detection in Ulaanbaatar using the breaks for additive seasonal and trend method. *Land*, *2*(4), 534–549. https://doi.org/10.3390/land2040534

Unal, Y. S., Toros, H., Deniz, A., & Incecik, S. (2011). Influence of meteorological factors and emission sources on spatial and temporal variations of PM10 concentrations in Istanbul metropolitan area. *Atmospheric Environment*, *45*(31), 5504–5513. https://doi.org/10.1016/j.atmosenv.2011.06.039

USGS. (2019). *Landsat 8-9 Operational Land Imager (Oli) - Thermal Infrared Sensor (Tirs) Level 2 (L2) Data Format Control Book (Dfcb)*. *2*(April), 1–64.

Verbesselt, J., Somers, B., Van Aardt, J., Jonckheere, I., & Coppin, P. (2006). Monitoring herbaceous biomass and water content with SPOT VEGETATION time-series to improve fire risk assessment in savanna ecosystems. *Remote Sensing of Environment*, *101*(3), 399–414. https://doi.org/10.1016/j.rse.2006.01.005

Verbesselt, Jan, Hyndman, R., Newnham, G., & Culvenor, D. (2010). Detecting trend and seasonal changes in satellite image time series. *Remote Sensing of Environment*, *114*(1), 106–115. https://doi.org/10.1016/j.rse.2009.08.014

Verbesselt, Jan, Hyndman, R., Zeileis, A., & Culvenor, D. (2010). Phenological change detection while accounting for abrupt and gradual trends in satellite image time series. *Remote Sensing of Environment*, *114*(12), 2970–2980. https://doi.org/10.1016/j.rse.2010.08.003

Verbesselt, Jan, Zeileis, A., & Herold, M. (2012a). Near real-time disturbance detection using satellite image time series. *Remote Sensing of Environment*, *123*(Turner 2010), 98–108. https://doi.org/10.1016/j.rse.2012.02.022

Verbesselt, Jan, Zeileis, A., & Herold, M. (2012b). Near real-time disturbance detection using satellite image time series. *Remote Sensing of Environment*, *123*, 98–108. https://doi.org/10.1016/j.rse.2012.02.022

Verbesselt, Jan, Zeileis, A., & Hyndman, R. (2015). Breaks For Additive Season and Trend (BFAST). Version 1.5.7. *Technical Report*. http://bfast.r-forge.r-project.org/

Vilà, M., Vayreda, J., Comas, L., Ibáñez, J. J., Mata, T., & Obón, B. (2007). Species richness and wood production: A positive association in Mediterranean forests. *Ecology Letters*, *10*(3), 241–250. https://doi.org/10.1111/j.1461-0248.2007.01016.x

Waller, E. K., Villarreal, M. L., Poitras, T. B., Nauman, T. W., & Duniway, M. C. (2018). Landsat time series analysis of fractional plant cover changes on abandoned energy development sites. *International Journal of Applied Earth Observation and Geoinformation*, *73*(March), 407–419. https://doi.org/10.1016/j.jag.2018.07.008

Wang, Y., Zhang, X., & Guo, Z. (2021). Estimation of tree height and aboveground biomass of coniferous forests in North China using stereo ZY-3 , multispectral Sentinel-2 , and DEM data. *Ecological Indicators*, *126*, 107645. https://doi.org/10.1016/j.ecolind.2021.107645

Watts, L. M., & Laffan, S. W. (2014). Effectiveness of the BFAST algorithm for detecting vegetation response patterns in a semi-arid region. *Remote Sensing of Environment*, *154*(1), 234–245. https://doi.org/10.1016/j.rse.2014.08.023

Wilson, E. H., & Sader, S. A. (2002). Detection of forest harvest type using multiple dates of Landsat TM imagery. *Remote Sensing of Environment*, *80*(3), 385–396. https://doi.org/10.1016/S0034-4257(01)00318-2

Wohlfart, C., Liu, G., Huang, C., & Kuenzer, C. (2016). A River Basin over the course of time: Multi-temporal analyses of land surface dynamics in the Yellow River Basin (China) based on medium resolution remote sensing data. *Remote Sensing*, *8*(3). https://doi.org/10.3390/rs8030186

Wu, L., Li, Z., Liu, X., Zhu, L., Tang, Y., Zhang, B., Xu, B., Liu, M., Meng, Y., & Liu, B. (2020). Multi-type forest change detection using BFAST and monthly landsat time series for monitoring spatiotemporal dynamics of forests in subtropical wetland. *Remote Sensing*, *12*(2), 1–33. https://doi.org/10.3390/rs12020341

Wulder, M. A., Masek, J. G., Cohen, W. B., Loveland, T. R., & Woodcock, C. E. (2012). Opening the archive: How free data has enabled the science and monitoring promise of Landsat. *Remote Sensing of Environment*, *122*, 2–10. https://doi.org/10.1016/j.rse.2012.01.010

Zeileis, A., Leisch, F., Kleiber, C., & Hornik, K. (2005). Monitoring structural change in dynamic econometric models. *Journal of Applied Econometrics*, *20*(1), 99–121. https://doi.org/10.1002/jae.776

Zhu, Z. (2017). Change detection using landsat time series: A review of frequencies, preprocessing, algorithms, and applications. *ISPRS Journal of Photogrammetry and Remote Sensing*, *130*, 370–384. https://doi.org/10.1016/j.isprsjprs.2017.06.013

Zhu, Z., & Woodcock, C. E. (2012). Object-based cloud and cloud shadow detection in Landsat imagery. *Remote Sensing of Environment*, *118*, 83–94. https://doi.org/10.1016/j.rse.2011.10.028

Zhu, Z., & Woodcock, C. E. (2014). Continuous change detection and classification of land cover using all available Landsat data. *Remote Sensing of Environment*, *144*, 152–171. https://doi.org/10.1016/j.rse.2014.01.011

Read, J. M., & Torrado, M. (2009). Remote Sensing. In *International Encyclopedia of Human Geography* (pp. 335-346). Elsevier. https://doi.org/10.1016/B978-008044910-4.00508-3

APPENDICES

APPENDIX A: BFAST code implementation in RStudio

Note: it is recommended that before starting check out correct version of "bfastspatial" from https://github.com/loicdtx/bfastSpatial. For more information and step by step tutorial about BFAST refer to http://changemonitor- wur.github.io/talks/bfastSpatial-2016/bfastSpatial_Peru.html#(1), http://www.loicdutrieux.net/bfastSpatial/ , and http://changemonitor-wur.github.io/deforestationmonitoring/ .

install developer's version of bfastSpatial, unless it has been updated to accommodate the new Landsat collection 1 data naming convention then no need for ref = 'develop' devtools::install_github('loicdtx/bfastSpatial', ref = 'develop').

```
#list of libraries, required for performing BFAST
library(raster)
library(rastervis)
library(sp)
library(usethis)
library(zoo)
library(xts)
library(forecast)
library(seas)
library(bfast)
library(devtools)
library(bfastSpatial)
library(lubridate)
library(ggplot2)
library(snow)
library(stringr)
library(parallel)

#set directory path
path <-'to-your-study-site-directory'

# load bfastSpatial and set tmpdir
tmpDir <- rasterOptions()$tmpdir

# set the path to the location of script
inDir <- file.path(path, 'data')

# stepDir is where intermediary outputs are stored
stepDir <- file.path(inDir, 'datastep')
```

```
# directory for Landsat data landsatDir
landsatDir <- file.path(stepDir, 'landsat')

# where individual VI layers are stored prior to being stacked; ndviDir, eviDir, etc.
are subdirectories of stepDir

ndviDir <- file.path(stepDir, 'ndvi')

ndmiDir <- file.path(stepDir, 'ndmi')

eviDir <- file.path(stepDir, 'evi')

nbrDir <- file.path(stepDir, 'nbr')

outDir <- file.path(inDir, 'out')

#to check out if your directories created successfully, if your directories created the
for loop fuction would excecute TRUE in RStudio.

for (i in c(stepDir, ndviDir, outDir, landsatDir)) {
  print(dir.exists(i))
}


#define each vegetation indices

.ndvi <- function() {
    ind <- c('band4','band5')
    fun <- function(x1, x2) {
        ndvi <- 10000 * (x2 - x1)/(x2 + x1)
        return(ndvi)
    }
    return(list(ind=ind,
                fun=fun))
}

.evi <- function() {
    ind <- c('band2','band4','band5')
    fun <- function(x1, x3, x4){
        evi <- 10000 * 2.5 * (x4/10000 - x3/10000)/(x4/10000 + 6 * x3/10000 - 7.5 *
x1/10000 + 1)
        return(evi)
    }
    return(list(ind=ind,
                fun=fun))

}

.nbr <- function() {
    ind <- c('band5','band7')
```

```
    fun <- function(x1, x2) {
        nbr <- 10000 * (x1 - x2)/(x1 + x2)
        return(ndvi)
    }
    return(list(ind=ind,
                fun=fun))
}

.ndmi <- function() {
    ind <- c('band5','band6')
    fun <- function(x1, x2) {
        ndmi <- 10000 * (x1 - x2)/(x1 + x2)
        return(ndvi)
    }
    return(list(ind=ind,
                fun=fun))
}
```

processLandsatBatch is variable due to the change in USGS ESPA file naming convention. If using developers version of bfastSpatial use the following to apply the cloud mask: keep = c(322, 386) applies to Landsat 8 data. Change to: keep = c(66, 130) for Landsat 5-7 data. Also, the purpose extent of the image shoul be defined as e in this process.

```
# processLandsatBatch, as an example for ndvi.
processLandsatBatch(x = landsatDir, outdir = ndviDir,  delete = TRUE, overwrite = TRUE, mask = 'pixel_qa', vi = 'ndvi', keep = c(322, 386), e= extent(xmin, xmax, ymin, ymax))

# before making temporal ndvi stack it is important to make a list of the layers.
ndviList <- list.files(outDir, pattern=glob2rx('ndvi*.grd'), full.names = FALSE)

#make temporal ndvi stack
ndviStack <- timeStack(x= ndviDir, pattern = glob2rx('*.grd'), filename = file.path(inDir, 'ndvi_stack.grd'), datatype = 'INT2S', overwrite=TRUE)

#in this section of code if it is matter to make a mask just from the forest area, first forest mask is defined as raster brick then x represented as multiple of ndviStack and the forest mask.

Forestmask<-brick (“the-forest-mask”)

#function set names is selected to be sure that layers name of ndviStack would not change after raster calculation.
x<-setnames (Forestmask*ndviStack, names (ndviStack))

# run bfmPixel() in interactive mode with a monitoring period
#bfmpixel would test to be sure there is a brek in monitoring period
```

```
library(snow)

bfm <- bfmPixel(x, start=c(monitoring period), interactive=TRUE, plot=TRUE)

#Click on a pixel in the plot.

#Plot the results
plot(bfm$bfm)

# run bfmSpatial on x/ndviStack with same parameters used in this research

# By default, 3 layers are returned: (1) breakpoint: timing of breakpoints detected for each pixel; (2) magnitude: the median of the residuals within the monitoring period; (3) error: a value of 1 for pixels where an error was encountered by the algorithm and NA where the method was successfully run.

bfm <- bfmSpatial( x,  pptype = 'irregular',  start =c(monitoring period), history = c(history period), type = "OLS-MOSUM", formula = response~harmon, order = 1, h=0.25, sensor= 'OLI', mc.cores = number of PC core wish to be used,  filename = file.path(outDir, 'bfm_ndvi_harmon.grd')...)

# optional: reformat sensor if needed

# prepare for subsetting

 sensor <- c(sensor, "ETM+ SLC-on", "ETM+ SLC-off", “OLI”)

s <- getSceneinfo(names(x))

s <- s[which(s$sensor %in% sensor), ]

# median values for all layers

if (!file.exists(fn <- file.path(outDir, 'medianVI.grd')))

   medVI <- summaryBrick(ndviStack, fun=median, na.rm=TRUE,

            filename = fn) else {

  medVI <- brick(fn)

}

plot(medVI/10000)

op<-par()
```

```
#post processing of bfm output
#load the bfm
bfm<- brick("directory to the bfm result")

#extract change raster
change <- raster(bfm, 1)

#convert breakpoint values to change months
months <- changeMonth(change)

# set up labels and colourmap for months
monthlabs <- c("jan", "feb", "mar", "apr", "may", "jun",
               "jul", "aug", "sep", "oct", "nov", "dec")
cols <- rainbow(12)
plot(months, col=cols, breaks=c(1:12), legend=FALSE)

# insert custom legend
legend("bottomright", legend=monthlabs, cex=0.5, fill=cols, ncol=2)

# extract magn raster
magn <- raster(bfm, 2)

# make a version showing only breakpoing pixels
magn_bkp <- magn
magn_bkp[is.na(change)] <- NA
op <- par(mfrow=c(1, 2))
plot(magn_bkp, main="Magnitude: breakpoints")
plot(magn, main="Magnitude: all pixels")
opar <- par(mfrow=c(1, 2))

# Write breakpoint, yearly break month product, and breakpoint magnitude raster
layers to GeoTiff files as well as the raster brick to a .grd fi
writeRaster(out[[1]], filename = "Site1_NDVI_breaks.tif", format = "GTiff",
overwrite = TRUE)
writeRaster(months$changeMonth2015, filename = "Site1_NDVI_breaksmos15.tif",
format = "GTiff", overwrite = TRUE)
writeRaster(months$changeMonth2016, filename = "Site1_NDVI_breaksmos16.tif",
format = "GTiff", overwrite = TRUE)
writeRaster(months$changeMonth2017, filename = "Site1_NDVI_breaksmos17.tif",
format = "GTiff", overwrite = TRUE)
writeRaster(months$changeMonth2018, filename = "Site1_NDVI_breaksmos18.tif",
format = "GTiff", overwrite = TRUE)
writeRaster(months$changeMonth2019, filename = "Site1_NDVI_breaksmos19.tif",
format = "GTiff", overwrite = TRUE)
writeRaster(months$changeMonth2020, filename = "Site1_NDVI_breaksmos20.tif",
format = "GTiff", overwrite = TRUE)
writeRaster(magn_bkp, filename = "Site1_NDVI_magbreaks.tif", format = "GTiff",
overwrite = TRUE) writeRaster(out, filename = "data/out/out_NDVI.grd", overwrite
= TRUE)
```

```
#Test breakpoints
plot(ndviStack[[80]], col = grey.colors(255), legend = F)
plot(out[[1]], add=TRUE)
#Test months product
plot(months, col=cols, breaks=c(1:12), legend=FALSE)
legend("bottomright", legend=monthlabs, cex=0.5, fill=cols, ncol=2)
#Test magnitudes plot(magn_bkp, main="Magnitude of a breakpoint")
plot(magn, main="Magnitude: all pixels")
```

CURRICULUM VITAE

PHOTO

Name Surname : Nooshin Mashhadi

Place and Date of Birth : Iran, 12.07.1993

E-Mail : mashhadi19@itu.edu.tr

EDUCATION :

- **B.Sc.** : 2016, BZTE University, Industrial Engineering

PROFESSIONAL EXPERIENCE AND REWARDS:

PUBLICATIONS, PRESENTATIONS AND PATENTS ON THE THESIS:

- Mashhadi, N., Alganci, U. 2021: Determination of forest burn scar and burn severity from free satellite images: a comparative evaluation of spectral indices and machine learning classifiers, International Journal of Environment and Geoinformatics (Basım İçin Kabul Aldı)

OTHER PUBLICATIONS, PRESENTATIONS AND PATENTS:

Mashhadi_MSC

ORIGINALITY REPORT

16%	12%	8%	3%
SIMILARITY INDEX	INTERNET SOURCES	PUBLICATIONS	STUDENT PAPERS

PRIMARY SOURCES

1	library.wur.nl Internet Source	2%
2	Vaughn Smith, Carlos Portillo-Quintero, Arturo Sanchez-Azofeifa, Jose L. Hernandez-Stefanoni. "Assessing the accuracy of detected breaks in Landsat time series as predictors of small scale deforestation in tropical dry forests of Mexico and Costa Rica", Remote Sensing of Environment, 2019 Publication	2%
3	www.mdpi.com Internet Source	1%
4	www.utupub.fi Internet Source	1%
5	ttu-ir.tdl.org Internet Source	<1%
6	portal.research.lu.se Internet Source	<1%
7	Submitted to University of Leicester Student Paper	<1%

8	Zhe Zhu. "Change detection using landsat time series: A review of frequencies, preprocessing, algorithms, and applications", ISPRS Journal of Photogrammetry and Remote Sensing, 2017 Publication	<1 %
9	en.wikipedia.org Internet Source	<1 %
10	repositorio.unb.br Internet Source	<1 %
11	researchbank.rmit.edu.au Internet Source	<1 %
12	Submitted to The Scientific & Technological Research Council of Turkey (TUBITAK) Student Paper	<1 %
13	e-space.mmu.ac.uk Internet Source	<1 %
14	d-nb.info Internet Source	<1 %
15	ftp.yzu.edu.tw Internet Source	<1 %
16	Submitted to Uskudar American Academy Student Paper	<1 %
17	landcover.usgs.gov Internet Source	<1 %

18	Al-Fares, Wafi(Hese, Sören and Schmullius, Christiane). "Historical Land use/Land cover classification and its change detection mapping using Different Remotely Sensed Data from LANDSAT (MSS, TM and ETM+) and Terra (ASTER) sensors : a case study of the Euphrates River Basin in Syria with focus on agricultural irrigation projects", Digitale Bibliothek Thüringen, 2012. Publication	<1 %
19	Submitted to University of Central England in Birmingham Student Paper	<1 %
20	polen.itu.edu.tr Internet Source	<1 %
21	www.calmit.unl.edu Internet Source	<1 %
22	Adrian Ochtyra, Adriana Marcinkowska-Ochtyra, Edwin Raczko. "Threshold- and trend-based vegetation change monitoring algorithm based on the inter-annual multi-temporal normalized difference moisture index series: A case study of the Tatra Mountains", Remote Sensing of Environment, 2020 Publication	<1 %
23	landsat.usgs.gov Internet Source	

		<1 %
24	edoc.ub.uni-muenchen.de Internet Source	<1 %
25	edepot.wur.nl Internet Source	<1 %
26	edoc.unibas.ch Internet Source	<1 %
27	www.usgs.gov Internet Source	<1 %
28	Submitted to University of Cape Town Student Paper	<1 %
29	opus.bibliothek.uni-wuerzburg.de Internet Source	<1 %
30	Submitted to University College London Student Paper	<1 %
31	horizon.documentation.ird.fr Internet Source	<1 %
32	Submitted to University of Edinburgh Student Paper	<1 %
33	ecommons.usask.ca Internet Source	<1 %
34	www.qucosa.de Internet Source	<1 %

35	www.tandfonline.com Internet Source	<1%
36	Schultz, Michael, Jan Verbesselt, Martin Herold, Valerio Avitabile, Daniel L. Civco, Karsten Schulz, Manfred Ehlers, and Konstantinos G. Nikolakopoulos. "Assessing error sources for Landsat time series analysis for tropical test sites in Viet Nam and Ethiopia", Earth Resources and Environmental Remote Sensing/GIS Applications IV, 2013. Publication	<1%
37	Submitted to Vels University Student Paper	<1%
38	eprints.lancs.ac.uk Internet Source	<1%
39	mdpi.com Internet Source	<1%
40	Chu, Thuan, and Xulin Guo. "Remote Sensing Techniques in Monitoring Post-Fire Effects and Patterns of Forest Recovery in Boreal Forest Regions: A Review", Remote Sensing, 2013. Publication	<1%
41	Jacob Mardian, Aaron Berg, Bahram Daneshfar. "Evaluating the temporal accuracy of grassland to cropland change detection	<1%

using multitemporal image analysis", Remote Sensing of Environment, 2021
Publication

42	Tingting He, Wu Xiao, Yanling Zhao, Wenqi Chen, Xinyu Deng, Jianyong Zhang. "Continues monitoring of subsidence water in mining area from the eastern plain in China from 1986 to 2018 using Landsat imagery and Google Earth Engine", Journal of Cleaner Production, 2021 Publication	<1 %
43	edoc.hu-berlin.de Internet Source	<1 %
44	eprints.soton.ac.uk Internet Source	<1 %
45	Submitted to Queen Mary and Westfield College Student Paper	<1 %
46	Submitted to RMIT University Student Paper	<1 %
47	Tulbure, Mirela G., and Mark Broich. "Spatiotemporal dynamic of surface water bodies using Landsat time-series data from 1999 to 2011", ISPRS Journal of Photogrammetry and Remote Sensing, 2013. Publication	<1 %

48	Zhe Zhu, Junxue Zhang, Zhiqiang Yang, Amal H. Aljaddani, Warren B. Cohen, Shi Qiu, Congliang Zhou. "Continuous monitoring of land disturbance based on Landsat time series", Remote Sensing of Environment, 2020 Publication	<1 %
49	iopscience.iop.org Internet Source	<1 %
50	mafiadoc.com Internet Source	<1 %
51	"Spatial Modeling in Forest Resources Management", Springer Science and Business Media LLC, 2021 Publication	<1 %
52	DeVries, Ben, Jan Verbesselt, Lammert Kooistra, and Martin Herold. "Robust monitoring of small-scale forest disturbances in a tropical montane forest using Landsat time series", Remote Sensing of Environment, 2015. Publication	<1 %
53	Khiry, Manal Awad (Prof. Dr. Joachim Hill, Prof. Dr. Marcus Nüsser, Prof. Dr. habil. Elmar Csaplovics and Technische Universität Dresden, Geowissenschaften). "Spectral Mixture Analysis for Monitoring and Mapping Desertification Processes in Semi-arid Areas	<1 %

in North Kordofan State, Sudan", Saechsische Landesbibliothek- Staats- und Universitaetsbibliothek Dresden, 2007.
Publication

54	creativecommons.org Internet Source	<1 %
55	www.sciencebuddies.org Internet Source	<1 %
56	Alexander Koltunov, Carlos M. Ramirez, Susan L. Ustin, Michèle Slaton, Erik Haunreiter. "eDaRT: The Ecosystem Disturbance and Recovery Tracker system for monitoring landscape disturbances and their cumulative effects", Remote Sensing of Environment, 2020 Publication	<1 %
57	J. Chen, J. Chen, J. Zhang. "A LANDSAT TIME-SERIES STACKS MODEL FOR DETECTION OF CROPLAND CHANGE", ISPRS - International Archives of the Photogrammetry, Remote Sensing and Spatial Information Sciences, 2017 Publication	<1 %
58	Michael Schultz, Jan G.P.W. Clevers, Sarah Carter, Jan Verbesselt, Valerio Avitabile, Hien Vu Quang, Martin Herold. "Performance of vegetation indices from Landsat time series in deforestation monitoring", International	<1 %

	Journal of Applied Earth Observation and Geoinformation, 2016 Publication	
59	Submitted to Wageningen University Student Paper	<1 %
60	EARTHDATA.NASA.GOV Internet Source	<1 %
61	Ipsita Nandi, Prashant K. Srivastava, Kavita Shah. "Floodplain Mapping through Support Vector Machine and Optical/Infrared Images from Landsat 8 OLI/TIRS Sensors: Case Study from Varanasi", Water Resources Management, 2017 Publication	<1 %
62	buildmedia.readthedocs.org Internet Source	<1 %
63	www.geosci-model-dev.net Internet Source	<1 %
64	peerj.com Internet Source	<1 %
65	thesis.univ-biskra.dz Internet Source	<1 %
66	www.forest.go.th Internet Source	<1 %
67	Pooja Gokhale Sinha. "chapter 2 Effect of Climate Change on Tropical Dry Forests", IGI	<1 %

Global, 2020
Publication

68	doi.org Internet Source	<1 %
69	lps16.esa.int Internet Source	<1 %
70	opendevelopmentmekong.net Internet Source	<1 %
71	ph338.edu.physics.uoc.gr Internet Source	<1 %
72	spie.org Internet Source	<1 %
73	www.eoearth.org Internet Source	<1 %
74	www.hydrol-earth-syst-sci.net Internet Source	<1 %
75	www.indiana.edu Internet Source	<1 %
76	www.int-arch-photogramm-remote-sens-spatial-inf-sci.net Internet Source	<1 %
77	www.safeproject.net Internet Source	<1 %
78	www2.db-thueringen.de Internet Source	<1 %

79	Aurélie C. Shapiro, Hedley S. Grantham, Naikoa Aguilar-Amuchastegui, Nicholas J. Murray et al. "Forest condition in the Congo Basin for the assessment of ecosystem conservation status", Ecological Indicators, 2021 Publication	<1 %
80	Meiling Liu, Xiangnan Liu, Ling Wu, Yibo Tang, Yu Li, Yaqi Zhang, Lu Ye, Biyao Zhang. "Establishing forest resilience indicators in the hilly red soil region of southern China from vegetation greenness and landscape metrics using dense Landsat time series", Ecological Indicators, 2021 Publication	<1 %
81	agritrop.cirad.fr Internet Source	<1 %
82	ascelibrary.org Internet Source	<1 %
83	eartharxiv.org Internet Source	<1 %
84	esajournals.onlinelibrary.wiley.com Internet Source	<1 %
85	espace.curtin.edu.au Internet Source	<1 %
86	link.springer.com Internet Source	

		<1 %
87	lup.lub.lu.se Internet Source	<1 %
88	publishup.uni-potsdam.de Internet Source	<1 %
89	refubium.fu-berlin.de Internet Source	<1 %
90	repository.kulib.kyoto-u.ac.jp Internet Source	<1 %
91	repository.up.ac.za Internet Source	<1 %
92	slidelegend.com Internet Source	<1 %
93	wiredspace.wits.ac.za Internet Source	<1 %
94	worldwidescience.org Internet Source	<1 %
95	www.acit2k.org Internet Source	<1 %
96	www.e-sciencecentral.org Internet Source	<1 %
97	www.loicdutrieux.net Internet Source	<1 %

98	www.pure.ed.ac.uk Internet Source	<1%
99	Chen, Lifan, Ryo Michishita, and Bing Xu. "Abrupt spatiotemporal land and water changes and their potential drivers in Poyang Lake, 2000–2012", ISPRS Journal of Photogrammetry and Remote Sensing, 2014. Publication	<1%
100	Liqin Yang, Qingyu Guan, Jinkuo Lin, Jing Tian, Zhe Tan, Huichun Li. "Evolution of NDVI secular trends and responses to climate change: A perspective from nonlinearity and nonstationarity characteristics", Remote Sensing of Environment, 2021 Publication	<1%
101	Arden L. Burrell, Jason P. Evans, Yi Liu. "Detecting dryland degradation using Time Series Segmentation and Residual Trend analysis (TSS-RESTREND)", Remote Sensing of Environment, 2017 Publication	<1%
102	Dengsheng Lu, Guiying Li, Emilio Moran. "Current situation and needs of change detection techniques", International Journal of Image and Data Fusion, 2014 Publication	<1%

103	Michael Schultz, Aurélie Shapiro, Jan Clevers, Craig Beech, Martin Herold. "Forest Cover and Vegetation Degradation Detection in the Kavango Zambezi Transfrontier Conservation Area Using BFAST Monitor", Remote Sensing, 2018 Publication	<1 %
104	philpapers.org Internet Source	<1 %
105	www.uts.edu.au Internet Source	<1 %
106	Li, Peng, Luguang Jiang, and Zhiming Feng. "Cross-Comparison of Vegetation Indices Derived from Landsat-7 Enhanced Thematic Mapper Plus (ETM+) and Landsat-8 Operational Land Imager (OLI) Sensors", Remote Sensing, 2013. Publication	<1 %

Exclude quotes	Off	Exclude matches	Off
Exclude bibliography	On		